



**National University of Science and Technology
POLITEHNICA Bucharest
Doctoral School of
Industrial Engineering and Robotics**

DOCTORAL THESIS

SUMMARY

*Contributions on increasing the durability of drill bits by welding
loading with high entropy alloys*

Violeta-Elena ȘTEFĂNESCU (PAVELIU)

Supervisor,

Prof.dr.ing. Ionelia VOICULESCU

INTRODUCTION

The doctoral thesis entitled, *CONTRIBUTIONS REGARDING THE INCREASE OF DRILL BITS' DURABILITY BY WELDING LOADING WITH HIGH ENTROPY ALLOYS*, falls within the field of industrial engineering and is based on a topical theme related to the reconditioning of heavily demanded drilling elements using new alloys, with special properties, called high entropy alloys. Exploitation of gas and fossil fuel reserves is a priority in the context of the new conditions for the purchase and consumption of petroleum products, generated by the economic crisis of energy resources at the European or global level. That is why the topic of the doctoral thesis is very current and important in this context. The PhD thesis presents the elements of designing and making high-entropy alloys from the AlCoCrFeNi and AlCrFeNiMn alloy systems to be used as filler materials for the welding loading of the wear zones of the drill bits.

In the first chapter presents the current status regarding the operating conditions and operational demands specific to drilling bits. The main types of drill bits used in drilling operations, the materials that are currently used for the manufacture of drill bits, the stresses they are subjected to during work, the areas where wear effects occur and the methods used for their reconditioning, the specific maintenance operations are presented and some conclusions defining the basic aspects related to the notions presented.

In the second chapter entitled "Methods and materials for the reconditioning of elements subjected to severe wear in the composition of drilling bits" presents in detail the main types of additive materials that are frequently used in welding loading of drilling bits, electrodes, wires and rods with chemical compositions that ensure high values of wear resistance characteristics. At the same time, the main methods used to carry out the refurbishment operations and the specific areas where the effects of intense wear appear are presented. The second part of the chapter presents the design principles of high entropy alloys, features specific of them, the main methods of obtaining them and fields of use recommended.

The third chapter presents the objectives and structure of the doctoral thesis, the research methods and equipment used to run the experimental program.

The fourth chapter contain experimental research carried out on laboratory-scale production of high-entropy alloys for welding loading of drill bits. Obtaining techniques and data on the chemical compounds and properties of the materials produced are presented. The fifth chapter, titled "Experimental research on the reconditioning by welding of worn out areas of the drilling bits", contains the results obtained by welding loading of worn out areas of the drilling bits. The sixth chapter, titled "Testing of samples loaded by welding" contains the tests and analyzes of microstructure, wear, hardness and corrosion resistance carried out on the samples taken from the areas loaded by welding. In the chapter titled "Conclusions and contributions, further research directions" the most relevant conclusions and original contributions resulting from the research activity are presented, as well as the directions on which future research will be oriented, after the completion of the doctoral thesis.

Contents of the Thesis Summary

Introduction	i
The content of the thesis	4
Theoretical part	
CHAPTER I.	
THE CURRENT STATE REGARDING THE OPERATING CONDITIONS AND OPERATIONAL REQUIREMENTS SPECIFIC TO OIL DRILL BITS	8
1.1. CONSTRUCTIVE FORMS OF DRILLING BITS	8
1.2. MATERIALS USED FOR THE MANUFACTURE OF DRILL BITS' ELEMENTS	8
CHAPTER II.	
METHODS AND MATERIALS FOR THE RECONDITIONING OF ELEMENTS SUBJECTED TO SEVERE WEAR IN THE COMPONENTS OF DRILL BITS	9
2.1. GENERAL ASPECTS REGARDING THE NEED TO RECONDITION DRILL BITS	9
2.2. TYPES OF MATERIALS USED FOR RECONDITIONING DRILL BITS	9
2.2.1. Coated electrodes	10
2.2.2. Wires for hard welding loads	10
2.3. METHODS OF LOADING HARD MATERIALS ON ACTIVE AREAS OF ROLLER DRILLS	10
2.3.1. Loading by welding of the teeth of the drill bits	10
2.3.2. Loading by welding the body of the jaws of the drill bits	10
2.4. DESIGNING OF HIGH ENTROPY ALLOYS FOR WELD LOADING OF DRILLING BITS	11
2.4.1. General aspects of high entropy alloys	12
2.4.2. Specific aspects of high entropy alloys	12
2.4.5. <i>Mechanical properties of high entropy alloys</i>	13
2.4.6. <i>Physical and chemical properties of high entropy alloys</i>	13
2.5. WELDING BEHAVIOR OF HIGH ENTROPY ALLOYS	14
2.5.1. <i>Electric arc welding of HEA</i>	14
2.6. CONCLUSIONS REGARDING THE WELDING BEHAVIOR OF HIGH ENTROPY ALLOYS	14
CHAPTER III.	
THE OBJECTIVES AND STRUCTURE OF THE DOCTORAL THESIS. RESEARCH EQUIPMENT	15
3.1. OBJECTIVES OF THE DOCTORAL THESIS	15
3.2. STRUCTURE OF THE DOCTORAL THESIS	15
3.3. RESEARCH APPARATUS USED TO CONDUCT THE EXPERIMENTAL PROGRAM	17

3.3.1. <i>The research equipment used to make the new high entropy alloys</i>	17
3.3.2. <i>The equipment used TO perform welded samples and heat treatments</i>	17
3.3.3. <i>Research equipment used to perform microscopy and surface characterization analyzes</i>	17
3.3.4. <i>Research equipment used to perform corrosion resistance tests</i>	17
3.3.5. <i>Research equipment used to perform wear tests</i>	17

Experimental part

CHAPTER IV.

EXPERIMENTAL RESEARCH ON THE LABORATORY SCALE OBTAINING OF HIGH ENTROPY ALLOYS FOR WELDING LOADING OF DRILLING PIPES	18
4.1. OBTAINING HEA ALLOYS	18
4.2. ANALYSIS OF THE MICROSTRUCTURE OF HIGH ENTROPY ALLOYS	22
4.2.1. <i>Analysis of alloys from the AlCrFeNiMn system</i>	22
4.2.2. <i>Analysis of high entropy alloys in the AlCoCrFeNi system</i>	2.3
4.3. CONCLUSIONS REGARDING THE OBTAINING AND CHARACTERIZATION OF THE NEW HIGH ENTROPY ALLOYS	27

CHAPTER V. EXPERIMENTAL RESEARCH REGARDING THE RECONDITIONING BY WELDING OF WORN OUT AREAS OF THE DRILLING BITS

5.1. WELDING PROCESSES APPLICABLE TO WELDING RECONDITIONING OF DRILL BITS	28
5.2. DESIGNING OF THE RECONDITIONING TECHNOLOGY THROUGH WELDING OF THE DRILLING BITS	28
5.2.1. <i>Analysis of worn out surfaces for welding loading purposes</i>	28
5.2.2. <i>Establishing the parameters of the welding regime</i>	28
5.3. RESEARCH ON THE DEPOSITION BY WIG WELDING OF HIGH-ENTROPY ALLOY ADDITION MATERIALS ON STEEL TAKEN FROM THE DRILL BIT	29
5.4. NON-DESTRUCTIVE EXAMINATION OF WELDED SAMPLES	30
5.4.2. <i>Examination with penetrant liquids</i>	30
5.5. DESTRUCTIVE TESTING	32
5.5.1. <i>Hardness level measurement</i>	32
5.6. PERFORMING EXPERIMENTS OF DEPOSITION OF HARD LAYERS WITH HIGH ENTROPY ALLOYS ON THE DRILLING BIT. THE SECOND BATCH	38
5.7. METALLOGRAPHIC ANALYSIS OF TIG WELDING DEPOSITS USING HIGH ENTROPY ALLOYS	39
5.8. CONCLUSIONS REGARDING THE WELD DEPOSITION BEHAVIOR OF HIGH ENTROPY ALLOYS ON DRILLING BITS	45

CHAPTER VI. TESTING OF WELDING LOADED SAMPLES

6.1. TRIBOLOGICAL ABRASION TESTS PERFORMED FOR DEPOSITS WELDED WITH HIGH ENTROPY ALLOYS	46
6.2. CORROSION RESISTANCE TESTING OF ALLOYS WELD DEPOSITED ON DRILLING BIT STEEL	49

6.3.	CONCLUSIONS REGARDING THE MECHANICAL AND CORROSION BEHAVIOR OF WELDED DEPOSITS FROM HIGH ENTROPY ALLOYS	50
------	---	----

CHAPTER VII. CONCLUSIONS AND CONTRIBUTIONS.	51
--	----

FURTHER RESEARCH DIRECTIONS	
------------------------------------	--

7.3.	PERSONAL CONTRIBUTIONS	51
------	------------------------	----

7.3.1 .	Theoretical contributions	51
---------	----------------------------------	----

7.3.2.	Scientific contributions	51
--------	---------------------------------	----

7.4.	FURTHER RESEARCH DIRECTIONS	51
------	-----------------------------	----

BIBLIOGRAPHY	52
---------------------	----

CHAPTER I. THE CURRENT STATE REGARDING THE OPERATING CONDITIONS AND OPERATIONAL REQUIREMENTS SPECIFIC TO OIL DRILL BITS

1.1. CONSTRUCTIVE FORMS OF DRILLING BITS

Drill bits are the most important components of drilling tools. They come into direct contact with the excavated material, which is why they are the most exposed elements of the drilling assembly, especially to the wear and corrosion stresses that occur in the process of making the borehole and removing the dislocated mineral material. [1-5].

Roller bits are specialized devices equipped with mobile elements, which are used to make oil well channels. [1-5].

Bits with three rollers (fig. 1.4.) are displacement tools composed of a central body, which by means of a spigot ensures the connection to the set of rods (2). It also has three massive jaws (1), on the axes of which the rollers (3) are fixed by means of bearings and sliding bearings. On the outside of the rollers are placed the cones made of hard materials (4) which break and remove the excavated rocks [10]. The rollers are prevented from moving along the axis by the ball bearing (6). The bearing balls are inserted through a channel made in the jaw, after which the supply area is sealed with a metal plug (7) that is welded. [8-10].

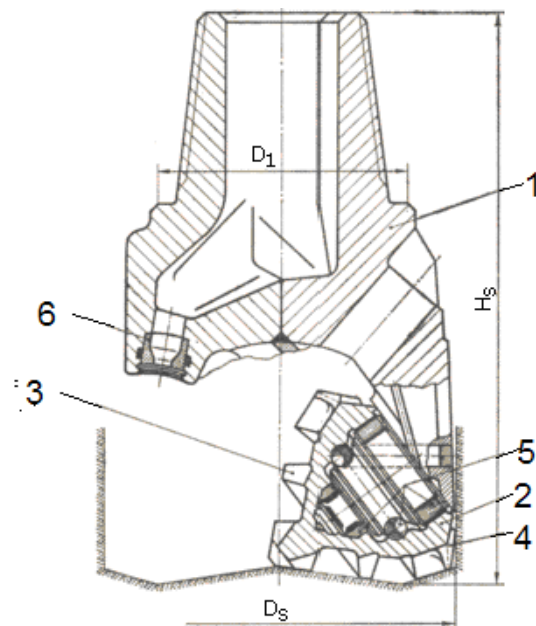


Fig. 1.3. Drill bit with external washing containing 3 tungsten carbide cones and rollers :
 1- the body of the bit; 2 – rolling cone; 3 – excavation pine; 4 – countercone; 5 – bearings;
 6 – channels for drilling fluid circulation;
 D_s – outer diameter; H_s – total height;
 D_1 – assembly diameter [8].

1.2. MATERIALS USED FOR THE MANUFACTURE OF DRILL BITS' ELEMENTS

The constructive elements of the drilling bits are, as a rule, made of different materials, chosen on the principle of maximum resistance to operational demands or on economic criteria (durability versus cost). [8-10]. The steels used for the manufacture of rotary cones (jaws) must have good weldability, therefore the current solution adopted is the use of alloy cementing steels, in which the percentage of carbon is limited (max. 0.2%C) to ensure the appropriate weldability.

CHAPTER II. METHODS AND MATERIALS FOR THE RECONDITIONING OF ELEMENTS SUBJECTED TO SEVERE WEAR IN THE COMPONENTS OF DRILLING BITS

2.1. GENERAL ASPECTS REGARDING THE NEED TO RECONDITION DRILLING BITS

Three-cone drills used for the creation of oil well channels work under severe conditions of abrasive wear and corrosion, which quickly causes the appearance of types of wear at the level of the main active elements.

In order to restore the geometry of the active areas of the drilling bits, a series of welding alloys have been developed that can be loaded, through different methods, on the worn out area. In situations where the wear is very high, it is recommended to apply reconstruction layers, this procedure being limited to about 3 superimposed hard layers. The filler materials used must cover various types of abrasion, corrosion or fatigue stress (fig. 2.2) [25-30].

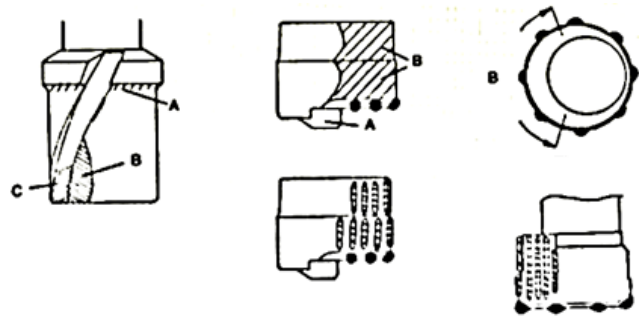


Fig. 2.2 . Examples of highly abrasion-stressed areas requiring reconditioning operations by welding loading [27].

2.2. TYPES OF MATERIALS USED FOR RECONDITIONING DRILLING BITS

Materials that are used for reinforcement or hard loading of bits can be classified as follows:

- Alloy steels with a content in alloying elements of less than 20% (Cr, Mn, Ni, V, W, B, etc.);
- Alloy steels with a content of alloying elements greater than 20% , which are much more expensive, but possess superior wear resistance compared to the first class of steels.
- Metal matrices belonging to various alloy systems: Cr, W, Co, Ni, V, Si, Zr, with different carbon contents. [39-44].
- Metal carbides embedded in metal matrices, which can be successfully used to reinforce or recondition worn areas. The most used are tungsten carbides, but also those of other elements, such as Cr, Ti, Ta, Mo, Va, Zr, Nb, which are embedded in metal binders based on Co, Ni, Cu, Mo, Ti, Ta [45-48]. For reinforcing the teeth of roller bits, the most used hard material is the Relit T-3 alloy (cast tungsten carbide, ground into granules) [50-55].
- High entropy alloys, which possess much higher mechanical characteristics compared to the chemical elements from which they are composed, such as: mechanical strength, resistance to wear and fatigue stress, hardness, toughness, which are attributed in particular to the ability to form complex and concentrated solid solutions, resulted by suppressing the tendency to form brittle intermetallic compounds. These alloys are characterized by the participation of at least 5 different chemical elements, introduced in equimolar proportions. [204].

2.2.1. Coated electrodes

Coated electrodes are used to restore the technological shape of heavily worn out areas, ensuring good accessibility to the areas of the jaws and the body of the drill bits (Fig. 2.3.). As can be seen from Fig. 2.3, first the 1, 2, 3 and 4 cords are laid on the diametrically opposite areas, then they are loaded, also diametrically opposite, on the 5, 6, 7 and 8 adjacent areas.

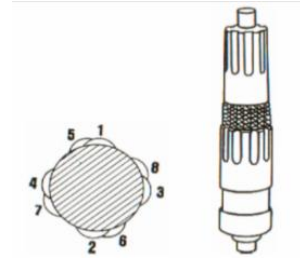


Fig. 2.3 . Exemple of the method of alternating deposition of welding cords on the components of drilling bits [5].

2.2.2. TIG welding rods

The 312 stainless steel rod for argon TIG welding is used in many applications, for dissimilar joints of manganese steels or for tools. These rods are used to restore the worn out shape of the parts.

2.3. METHODS OF LOADING HARD MATERIALS INTO THE ACTIVE ZONES OF ROLLER DRILL BITS

2.3.1. Loading by welding of the teeth of the drill bits

To increase the durability of the working surface of the cones of roller bits, the teeth can be loaded with hard material. Hard alloy layers can be deposited by welding with oxyacetylene flame, with an electric arc, plasma or with a laser.

The teeth in the central area of the rollers are partially or fully loaded, on both sides. In general, bit teeth are reinforced according to their purpose. For bits intended for the processing of channels in hard rocks, both edges of the teeth are reinforced, on their entire height, the deposits being made on the peripheral crown, on all three edges of the tooth (fig. 2.9).



Fig. 2.9 . Image of the core area of a three-roller drill bit with advanced tungsten carbide insert wear [11].

2.3.2. Loading by welding the body of the jaws of the drill bits

The body of the jaws is the area that interacts with the walls of the borehole, being mainly subjected to abrasion wear. In 3-roller bits, the jaws are positioned and fixed by welding (fig. 2.10). To protect the welded seams, the surface of the body can be loaded with hard material, to a height of between 85-100 mm, on the areas at the front of the bit.

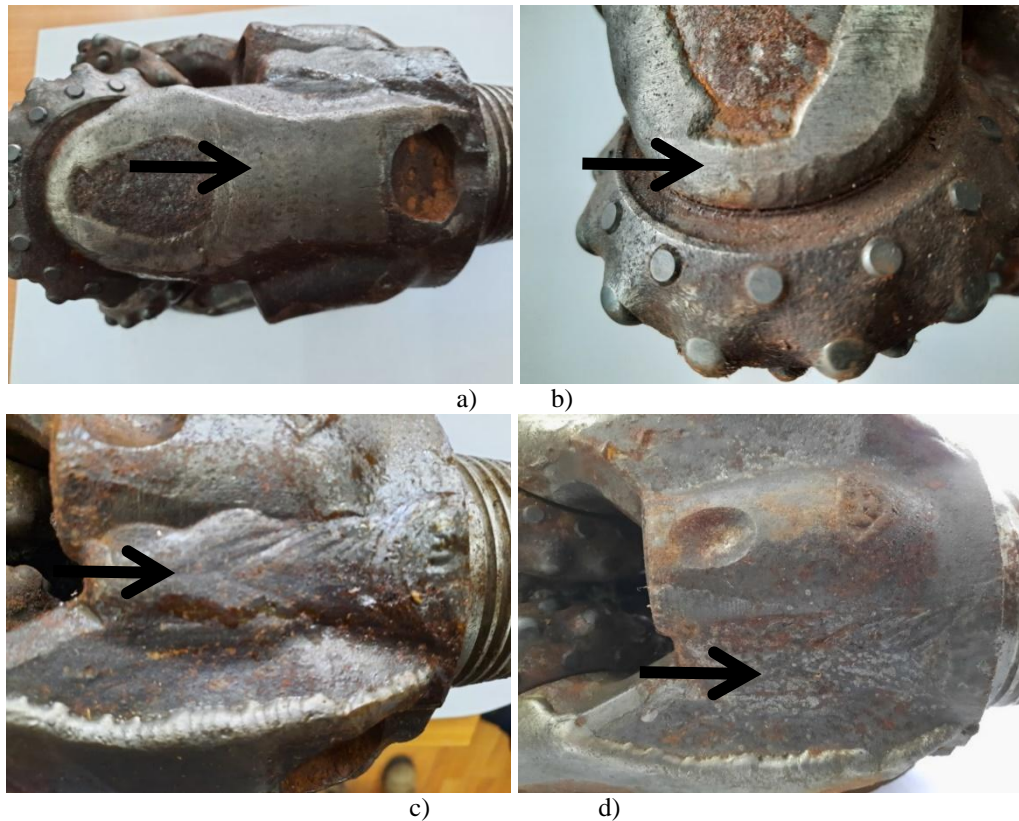


Fig. 2.10 . Welded areas where hard metal was deposited by welding at the drill bits.
 a) overview of the side loading area; b) detail on the side loading area; c) hard loading area over the bit jaw assembly weld;
 d) the hard loading area on the lateral flanks of the drill bit jaws .

The research in this doctoral thesis focused on the performance of the clamping welds of the jaws of the drilling bits, for the geometric calibration of the jaws, in the event of the appearance of some wear that causes them to be taken out of use. The presented solution can also be used for other areas of interest, including the remake of tip or support areas.

2.4. DESIGNING OF HIGH ENTROPY ALLOYS FOR WELD LOADING OF DRILLING BITS

HEA alloys have caused a *revolution* in the field of materials' science due to their great potential for use as functional and structural materials. HEAs have at the same time very good mechanical properties, such as high hardness levels, but also the ability to maintain their mechanical strength at high temperatures, which is extremely important in the aerospace industry. Experiments conducted have shown that certain HEAs have excellent resistance to oxidation, wear and corrosion.

The equilibrium of the metallurgical system of the alloys can be obtained for minimum values of the free energy (G), according to the relation proposed by Gibbs (2.1):

$$G=H-TS, \text{ or } \Delta G_{mix}=\Delta H_{mix}-T\Delta S_{mix} \quad (2.1)$$

where G is the free energy (or Gibbs enthalpy), H - enthalpy, T - temperature and S - entropy.

According to the hypothesis proposed by Boltzmann, the mixing entropy of an alloy that has completely equiatomic proportions of n -elements, when passing from the elementary solid solution to the random (ideal) solution stage, can be calculated using equation 2.3:

$$\Delta S_{mix} = R \cdot \ln(n) \quad (2.3)$$

where R is the ideal gas constant, equal to $8.314 \text{ J} \cdot \text{mol}^{-1} \cdot \text{K}^{-1}$.

For the number of participating elements between $n=5$ and $n=13$, entropy values between $1.61R$ and $2.56R$ are obtained, being located in the so-called domain of high entropy alloys.

Thus, the energy difference between these alloys can be highlighted (Fig. 2.11).

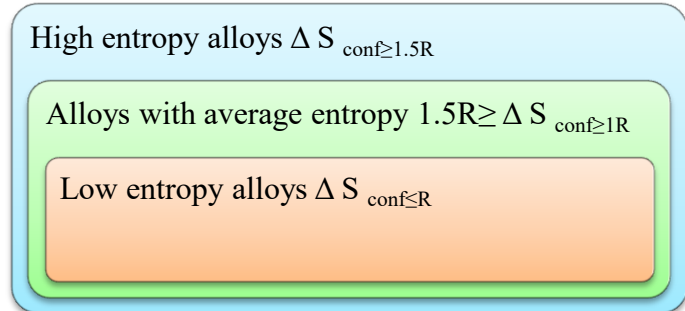


Fig. 2.11. Ranges of entropy values for alloys (According to Murty B. S. et al.) [19].

2.4.1. Specific aspects of high entropy alloys

Researcher J. W. Yeh formulated four "basic effects" that occur in high-entropy alloys containing different atoms, which significantly affect the properties of the materials. These are called high entropy, distortion of dislocation lines, slow diffusion and cocktail effects.

2.4.2. Methods of creating high entropy alloys

a. Melting via an electrical arc in a vacuum

Obtaining high-entropy alloys by melting high-purity raw materials in furnaces equipped with either electrical resistance or induction systems is a practice already developed on a laboratory scale. The advanced vacuum level ($10^{-2} \div 10^{-4}$ torr) during the melting period ensures optimal gas evacuation conditions, but facilitates the evaporation of easily fusible elements, which cannot be used in these metallurgical aggregates (fig. 2.15). The ingots or the mini-ingots obtained with these furnaces have a dendritic structure, with columnar grains that form and grow equiaxially in the direction of the heat flow (fig. 2.16).

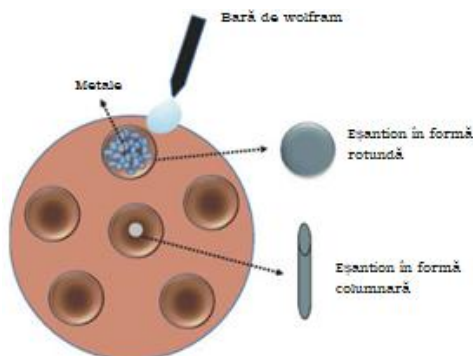


Fig. 2.15 . Principle diagram of the remelting process via an electrical arc in a vacuum



Fig. 2.16 . Equiaxial grainning in a high-entropy AlCrFeMnNi ingot [16].

b. Melting in an electric induction furnace

The induction furnace is a metallurgical aggregate in which ferrous and/or non-ferrous metal alloys are obtained from materials and alloys of commercial purity, with low phosphorus and sulfur contents, by melting under the action of induction currents, through the Joule – Lenz effect (fig. 2.17). The melting of metallic materials is carried out in a ceramic crucible (either basic or acidic).

2.4.5. Mechanical properties of high entropy alloys

❖ The tensile/compressive behavior and hardness

In 2014, Wu et al. studied the mechanical properties of the family of equiatomic quaternary, ternary and binary alloys with compositions containing Fe, Co, Ni, Cr and Mn. In figure 2.23, some values of the hardness determined by studies performed on HEA type alloys are presented, compared to classical alloys. Zhang et al. [130] showed that rapid solidification after surface laser melting produced a relatively high hardness of 1152 HV in FeCoNiCrCuTiMoAlSiB_{0.5} alloy.

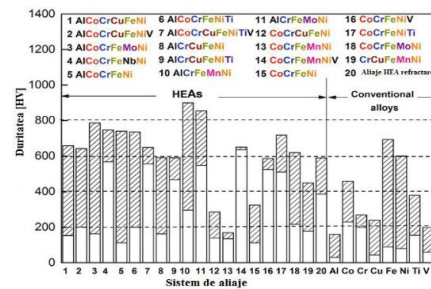


Fig. 2.23. Hardness values of some HEA alloys compared to conventional alloys [12].

❖ Wear resistance of high entropy alloys

Figure 2.26. presents an analysis of wear resistance values in the case of the high entropy alloy Al_{0.5}B_xCoCrCuFeNi, by comparison with traditional alloys.

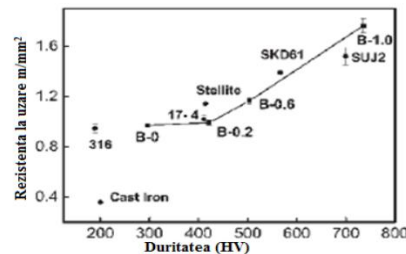


Fig. 2.26. Effect of boron content in Al_{0.5}B_xCoCrCuFeNi alloy on wear resistance and hardness [125].

2.4.6. Physical and chemical properties of high entropy alloys

❖ Magnetic properties

Studies on the magnetic properties of HEAs are mainly focused on alloys derived from the Al-Mn-Cr-Cu-Co-Fe-Ni-Ti systems. These alloys contain more than 50% magnetic elements (Fe, Co and Ni). They are either paramagnetic or ferromagnetic with a magnetization saturation (Ms) typically around 10–50 emu/g (if converted to weighted average density, roughly in the range of 70–350 emu/cc). [146-150].

❖ Thermal properties

Thermal conductivity/diffusivity was determined for Al_xCoCrFeNi and Al_xCrFe_{1.5}MnNi_{0.5}M_{0y} alloys, establishing that the thermal conductivity value of Al_xCoCrFeNi falls within the range of 10⁻²⁷ W/m·K. [153].

❖ Oxidation resistance of HEA alloys

The oxidation resistance of alloys can be increased by adding elements such as Al, Cr, and Si, which have the ability to form an impenetrable, dense, adherent and stable oxide layer on the surface of the alloy that protects it from the action of oxygen at high temperatures . [131-138].

❖ Change in hardness with temperature

Many HEA alloys have exceptional mechanical strength and hardness at high temperatures, which ensure their excellent behavior under thermal stress. $\text{AlCoCr}_2\text{FeMo}_{0.5}\text{Ni}$ and $\text{Al}_{0.2}\text{Co}_{1.5}\text{CrFeNi}_{1.5}\text{Ti}$ alloys have a very high hardness level at room temperature, but its value decreases slowly with increasing temperature (Fig. 2.28.)

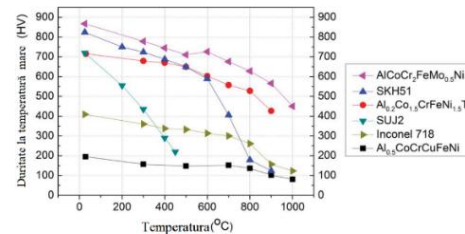


Fig. 2.28. Hardness of various HEAs and conventional alloys based on different temperature levels [106].

❖ Corrosion resistance of HEA

The corrosion resistance of metals and alloys depends on several factors, such as chemical composition, temperature, working environment and microstructure. $\text{FeTa}_{0.5}\text{Nb}_{0.5}\text{Ti}_{1.5}\text{Zr}_{0.5}$ exhibits better corrosion resistance than Ti-6Al-4V, which can be mainly attributed to the addition of Nb, Ta and Zr elements in the alloy, leading to the formation of a more stable and inert layer of oxide (mainly composed of TiO_2 , Nb_2O_5 , NbO_2 , Ta_2O_5 and ZrO_2) on the surface of the $\text{FeTa}_{0.5}\text{Nb}_{0.5}\text{Ti}_{1.5}\text{Zr}_{0.5}$ alloy. The addition of Ta can improve the strength resistance of Ti alloys in chlorine solutions because pure Ta is resistant to chlorine due to the relative stability of the Ta_2O_5 oxide solution.

2.5. WELDING BEHAVIOR OF HIGH ENTROPY ALLOYS

2.5.1. Electric arc welding of HEA

Electric arc welding is one of the most common welding methods, in which the energy developed by its combustion simultaneously melts the surface of the parts and a consumable filler material (coated electrode, wires or rods), with or without a protective atmosphere. There are several welding processes applicable to HEA joining, the best known being: shielded metal arc welding (SMAW), gas tungsten arc welding (GTAW) (also known as TIG - Tungsten inert gas), gas metal arc welding (GMAW), flux-cored arc welding (FCAW or FCA), submerged arc welding (SAW). [216, 217] .

2.6. CONCLUSIONS REGARDING THE WELDING BEHAVIOR OF HIGH ENTROPY ALLOYS

❖ High-entropy alloys possess properties superior to classical alloys, such as very high mechanical strength resistance, considerable hardness, high wear resistance, and exceptional toughness at high or very low temperatures. By definition, HEAs with c.f.c. structure are more ductile, being characterized by a relatively low crystal network strain. As a result, these alloys are not prone to cracking and abnormal diffusion behavior.

CHAPTER III. THE OBJECTIVES AND STRUCTURE OF THE DOCTORAL THESIS. RESEARCH EQUIPMENT

3.1. OBJECTIVES OF THE DOCTORAL THESIS

The choice of the topic of the doctoral thesis is related to the importance of the field of new materials used for welding reconditioning of drill bits, which allow to increase the life expectancy of such a tool. AlCrFeMnNi class alloys are characterized by very high wear resistance up to temperatures of 800 °C, as a result of hardness values of up to 800-900 HV, obtained by thermal annealing treatments for homogenization and quenching in water. Based on previous bibliographical studies, chemical composition limits were established for high-entropy alloys in the AlCrFeMnNi and AlCoCrFeNi systems that were used for weld loading of drill bits to increase service life. The theoretical researches were focused on achieving the following major objectives:

- The study of the basic notions of drill bits, including types and dimensions, application conditions, materials used for their manufacture, maintenance operations and specific problems.
- Knowledge of the main techniques and materials used for the reconditioning of elements subject to severe wear and tear in the composition of drilling bits.

The experimental research aimed to achieve the following objectives:

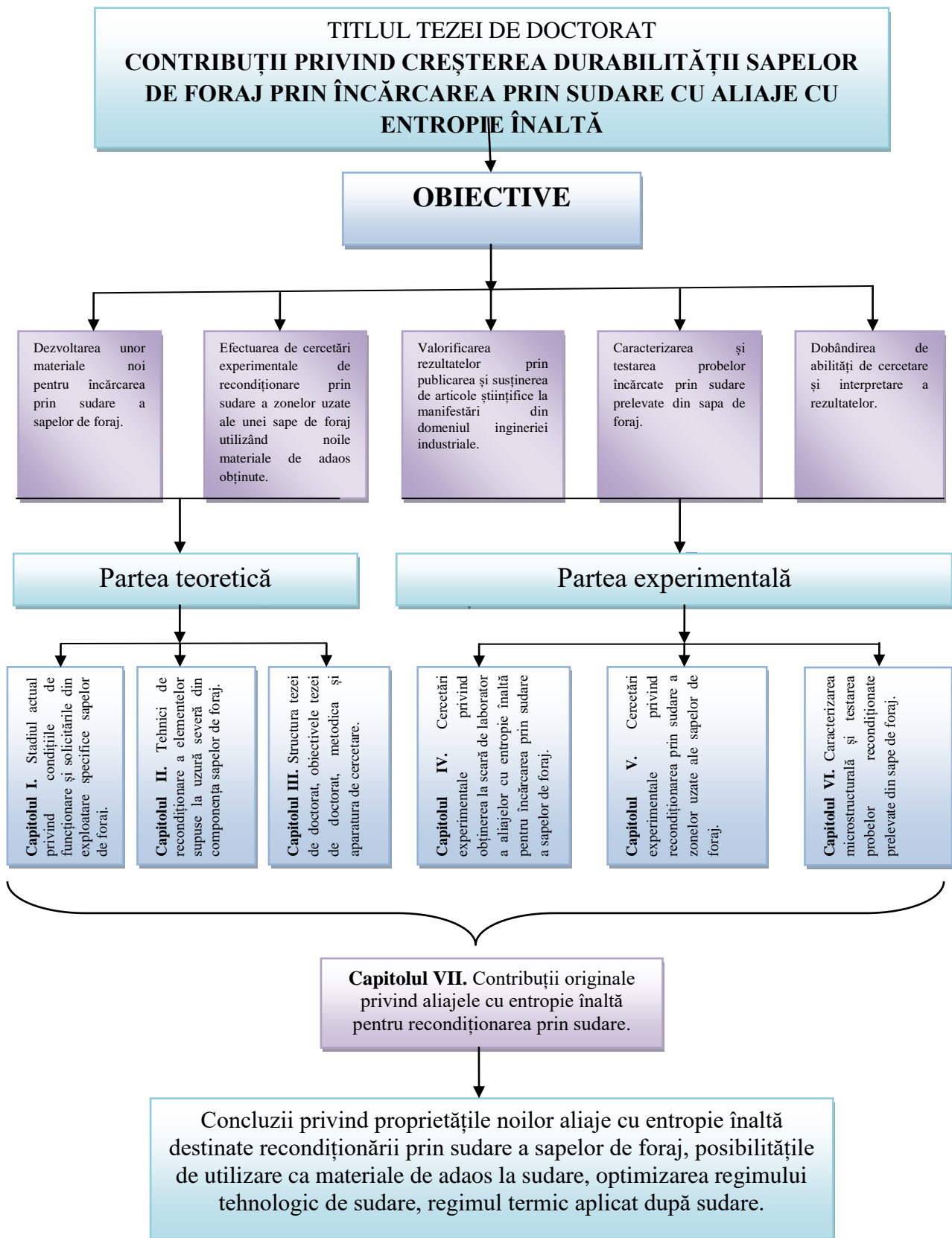
- The development of new materials for the welding loading of drill bits, which simultaneously possess high values of hardness, wear resistance and corrosion, to be able to withstand the complex stresses during the soil excavation process;
- Carrying out experimental research on reconditioning by welding the worn areas of a drill bit using the new additive materials obtained;
- Characterization and testing of weld loaded samples taken from the drill bit;
- Capitalizing on the results by publishing and supporting scientific articles at events in the field of industrial engineering;
- Acquisition of research skills and interpretation of results, training by study, applied and experimental research of the PhD student.

3.2. STRUCTURE OF THE DOCTORAL THESIS

In order to achieve the objectives proposed within the doctoral improvement activity, a plan was drawn up for carrying out all study, documentation, experimentation and testing activities, capitalizing on the results by publishing papers or participating in scientific communication conferences. This plan is shown schematically in fig. 3.1.

As can be seen in fig. 3.1, the first stage of the research plan consisted in the theoretical preparation, by studying and deepening the basic notions regarding the elements considered for reconditioning, i.e. drill bits, including types and dimensions, demand conditions, materials used for their manufacture, maintenance operations and specific problems.

The theoretical training continued by studying the main techniques for reconditioning the drill bits used at the industrial level, in order to be able to withstand the specific demands from exploitation.



3.3. RESEARCH APPARATUS USED TO CONDUCT THE EXPERIMENTAL PROGRAM

Experimental research was carried out to obtain high-entropy alloys from the AlCrFeMnNi alloy system and from the AlCoCrFeNi alloy system, from which the welding loading rods were made on a laboratory scale. The determination of the chemical composition of the high entropy alloy batches was carried out using the spark optical emission spectrometer and through EDAX analyzes. The new filler materials obtained were then used for welding loading directly on the wear surfaces of a drill bit, as well as on areas sampled from it.

3.3.1. The research equipment used to make the new high entropy alloys

The new high-entropy alloys were designed and made in the ERAMET laboratory at the SIM Faculty, UPB, using: RAV – MRF ABJ 900 Installation and KERN ABJ Analytical Scale, with measurement precision $\epsilon = 1\text{mg}$.

3.3.2. The equipment used to perform welded samples and heat treatments

The welded samples were made in the Welding laboratory of the Department of Quality Engineering and Industrial Technologies, IIR Faculty, UPB using the TIG PRESTOTIG 210 welding source and Nabertherm Furnace.

3.3.3. Research equipment used to perform microscopy and surface characterization analyzes

The analyzes of the microstructures of the metal surfaces were carried out in the LAMET laboratory, from UPB, Department of Quality Engineering and Industrial Technologies, IIR Faculty, Polytechnic University of Bucharest, Room CK106 using the scanning electron microscope (SEM) Quanta Inspect S, FEI Netherlands, Type FP201711, equipped with EDAX AMETEC Z2e analyzer, OLYMPUS GX51 optical microscope, equipped with AnalySIS image processing system, Shimadzu HMV2T microdurometer, Japan, machine for precision sampling of metallographic samples - ISOMET 4000 Buehler, machine for automatic grinding and polishing of metallographic samples - Vector and Buehler Alpha Beta polisher, UCI 50 ultrasonic cleaning system.

3.3.4. Research equipment used to perform corrosion resistance tests

The corrosion resistance was determined in the Electrochemistry and Surface Functionalization Laboratory - ElectroSurF, JK209, SIM, UPB, by the linear polarization technique (Potentiostat/ Galvanostat (type PARSTAT 4000, AMETEK, USA).

3.3.5. Research equipment used to perform wear tests

The tribological properties were determined by wet abrasion, on the surfaces loaded by welding (mechanically processed and polished with fine abrasive paper), in the Metrology laboratory, from the Mechanics Faculty, UPB. For each type of sample, five successive tribological tests were performed (Apparatus for determining wear resistance Plint 66).

CHAPTER IV. EXPERIMENTAL RESEARCH ON THE LABORATORY SCALE OBTAINING OF HIGH ENTROPY ALLOYS FOR WELDING LOADING OF DRILLING PIPES

4.1. OBTAINING HEA ALLOYS

The special mechanical properties of the alloys in the AlCrFeMnNi and AlCoCrFeNi alloy systems can be adjusted by the appropriate modification of the chemical composition, especially by changing the aluminum content [147-150]. The chemical elements in the alloys belonging to the AlCoCrFeMnNi alloying systems, such as Cr, Ni and Al, also greatly influence the corrosion behavior, which can be taken into account when establishing the material networks, depending on their possible applications for additive manufacturing intended for hard loading of drill bits [151-162]. The surfaces to be loaded by welding with filler materials from high-entropy alloys require more careful mechanical preparation, so as to avoid contamination of the weld with elements of type C, S, P that may come from residues from oxide crusts or organic contaminants [168,169].

Based on previous bibliographical studies, chemical composition limits for high-entropy alloys in the AlCrFeMnNi and AlCoCrFeNi systems to be used for weld loading of drill bits have been established in this chapter, with the purpose of increasing service life and analyzing replacement possibilities of the expensive Stellite-type alloys currently in use. The preliminary tests regarding obtaining the high entropy alloys from the Al_xCrFeMnNi and Al_xCoCrFeNi alloy systems were carried out in the **ERAMET laboratory** (www.eramet.ro) of the SIM Faculty of the Polytechnic University of Bucharest, using the arc remelting facility in a vacuum, type MRF ABJ 900 (Fig. 4.1) .

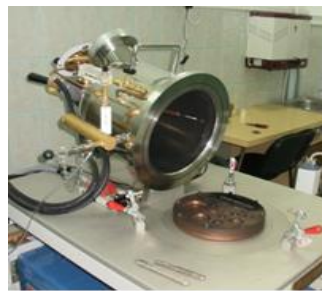


Fig. 4.1. The RAV – MRF ABJ 900 facility with which the experimental high entropy alloys were obtained. ERAMET Laboratory, UPB.

The raw materials used to obtain these alloys were of advanced purity and were selected on the basis of chemical composition and granulation, so that they could be easily placed in the melting recesses (calibrated cells made in the water-cooled copper plate of the facility). The

preparation of the raw materials and the distribution of the elements of the metal load on the melting plate of the RAV plant is shown in fig. 4.2.



Fig. 4.2. Preparation of raw materials (a) and distribution of metal charge elements on the melting plate in the RAV facility (b).

The melting was achieved with the help of the electric arc started between a tungsten electrode alloyed with 2% Th and the metal charge. This was in the form of granules or plates with a maximum size of 10mm and was loaded into the special copper plate recesses of the facility, which is force cooled by water to avoid common melting and alloying with the elements of the charge during their processing. To ensure a high homogeneity of the alloys, the charge was remelted several times, on each side (minimum 5 - 7 times). An example of $Al_xCrFeMnNi$ alloy obtained after the elaboration and solidification process is shown in fig. 4.3. The uneven surface of the obtained bar can be observed, which copied the shape of the recess where the solid raw materials were melted. That's why, after cooling, this mini-ingot was subjected to mechanical processing operations, through which the superficial crusts of oxides were removed and the size required for welding deposition was obtained.



Fig. 4.3. S2 HT3 – AlCrFeMnNi alloy mini-ingot.

The calculation of the charge of the high-entropy alloys in the AlCrFeMnNi system was carried out in order to achieve equiatomic proportions of participation for each chemical element, the values obtained by calculation being reproduced in Tab. 4.1.

Chart 4.1. Load calculation corresponding to the alloy S2 HT 3 - $Al_{0.5}CrFeMnNi$
 $Al_{0.5}CrFeMnNi$ alloy (Molar mass= 235.5 g)

S2 HT 3 Charge		Element					Load weight, g	Charge efficiency, Mr
		Al	Cr	Fe	Mn	Ni		
		Weight, %	5.71	22.02	23.76	23,34		
Weight, g	5.16	19.87	21.40	21.01	22.56			

As can be seen from the efficiency value for the batch of high entropy alloy called HT, a mass loss of about 1.9 g was recorded, most likely due to the evaporation of the Al, Mn, Fe, Cr chemical elements, which have higher evaporation rates specific values compared to Ni.

After obtaining the new alloys in the RAV facility, the alloy was obtained using the Balzers vacuum induction furnace type HU-40-25-40-04, from the ERAMET Laboratory of the SIM Faculty, UPB.

Crucibles made of MgO and dry refractory mass type Rodacor Mix 016, which is a chemically neutral material, which allows the formation of neutral spinels at temperatures between 1650 - 1700°C, were used for the preparation and casting of the HT 3 alloy batches. The preparation for the crucible (stamping) followed, and sintering was carried out at a speed of about 200 °C/h.

The loading order in the induction furnace was as follows: ARMCO type iron, nickel, chromium, manganese and in the end aluminium. Al is added to the melt before it is poured into the molds, which are preheated beforehand. After casting the HT 3 alloy, a period of about 2 hours was left for the solidification and cooling of the cast alloys, then the rods were extracted, the surfaces were cleaned and disconnected from the supply networks (fig. 4.5).

To determine the chemical composition of the high-entropy alloy batches, the spark optical emission spectrometer - SPECTROMAXx M, was used in the LISEOFRX laboratory (www.liseofrx.ro), from the SIM Faculty, UPB. Part of the analysis was carried out by comparison with the AMETEC Z2e analyzer, equipped with the SEM Quanta Inspect S electronic microscope, from the LAMET laboratory, UPB. The chemical composition analysis was performed using two programs specific to nickel base alloys (Ni-01) and steels (Fe-01), the results being approximate. The simplified chemical composition determined for the HT3 alloy batch was as follows: Al ≈ 5.2 %; Cr ≈ 23.29%; Fe ≈ 23.36%; Mn ≈ 23.8%; Ni ≈ 23.50%; Other elements = 0.85%.



In order to be able to be used in good conditions for melting and deposition by welding, the rods cast from the experimental alloys were mechanically processed by turning, obtaining rods with a length of 160 mm and a diameter of 4 mm (fig. 4.6).

Fig. 4.6. S2 HT 3 alloy rods resulted from mechanical processing by turning.

High entropy alloys from the $AlxCoCrFeNi$ system were obtained following a similar procedure. These alloys are characterized by high compressive strength resistance (2004 MPa), high values of flow and breaking resistance strengths (1250

MPa), good values of breaking energy at 20 ° C (60-62 J) and high hardnesses (350 – 650 HV0.2), which depend on the alloy level and delivery condition [177].

The atomic masses of the elements used to obtain the high-entropy alloys were as follows: Al=27 g/mol; Cr = 52 g/mol; Fe = 56 g/mol; Co = 59 g/mol; Ni = 59 g/mol. The chemical compounds of the batches made of HEA alloys from the AlCoCrFeNi system are presented in the 4.2 chart and the appearance of the mini-ingots obtained in fig. 4.7.

Chart 4.2. Chemical compound of the experimental alloys in the AlCoCrFeNi system

Alloy		Element					load mass, g
		Al	Cr	Fe	Co	Ni	
Alloy HEA 1 AlCoCrFeNi Molar mass M _{mol.} = 253 g	Mass percent, %	10.67	20.55	22.13	23.32	23.33	200.82
	mass, g	22	41.04	44.24	46.64	46.9	
	Molar mass, % at.	20	20	20	20	20	
Alloy HEA 5 Al _{0.8} CoCrFeNi Molar mass M _{mol.} = 247.6 g	Mass percent, %	8.72	21	22.61	23.82	23.85	52,53
	mass, g	4.57	11.01	11.85	12.5	12.6	
	Molar mass, % at.	20	20	20	20	20	
Alloy HEA 6 Al _{0.6} CoCrFeNi Molar mass M _{mol.} = 242.2 g	Mass percent, %	6.68	21.47	23.12	24.36	24.36	79.9
	mass, g	5.34	17,17	18.5	19.49	19.4	
	Molar mass, % at.	20	20	20	20	20	



Fig. 4.7. Appearance of mini-ingots obtained from AlCoCrFeNi alloys.

For the characterization of the experimental alloys, samples were taken from the obtained micro-ingots, using the IsoMet 4000 high-precision cutting machine (LAMET Laboratory, UPB). The cutting parameters used were: speed: 2050 rpm; cutting advance speed: 5.5mm/min; disc type: extruded materials (R/Al2O3).

From each high-entropy alloy mini-ingot, small end portions were cut, with a thickness of about 10mm. Then, the alloy samples were hot embedded, using phenolic resin (PhenoCure) (fig. 4.10), at a temperature of 195 ° C. The surfaces of the alloys were sanded with abrasive papers

with progressive grits (600 – 2500) and then they were polished with abrasive alumina powder (granulation 10 – 0.1 μm).



Fig. 4.10. Appearance of AlCrFeMnNi alloy samples after embedding in resin.

After metallographic preparation, the samples were washed with ethanol in an ultrasonic bath, dried and then chemically attacked with 10% oxalic acid for optical and electron microscope analysis.

4.2. ANALYSIS OF THE MICROSTRUCTURE OF HIGH ENTROPY ALLOYS

4.2.1. Analysis of alloys from the AlCrFeNiMn system

The microstructure analyzes were carried out by SEM scanning electron microscopy, with the Inspect S electron microscope, FEI Netherlands, equipped with the EDAX analysis system, AMETEC Z2e, for visualizing the fracture surfaces (fig. 4.11 – 4.13).

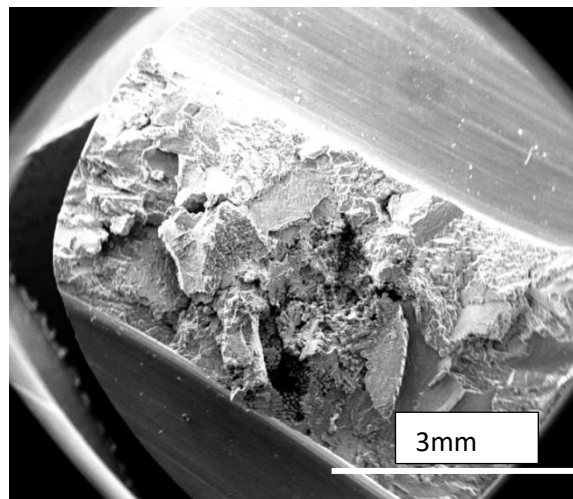


Fig. 4.11. The appearance of the fracture surface in the HT alloy 3. SEM microscopy. LAMET laboratory.

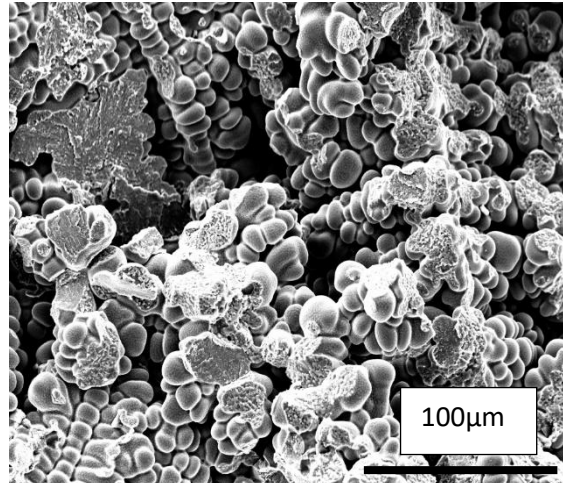


Fig. 4.12. SEM analysis of the central area of the HT 3 alloy mini-ingot. Solidified dendrites and brittle fracture surfaces. LAMET laboratory.

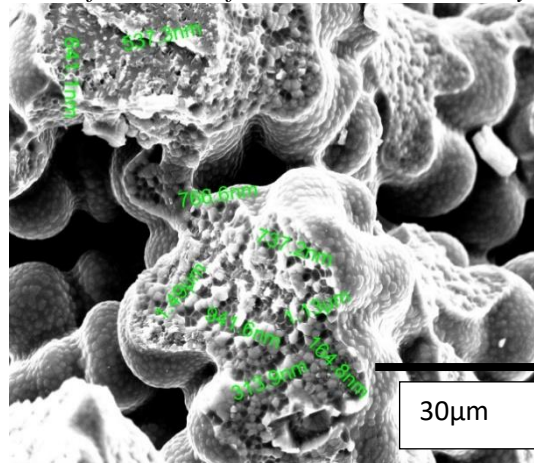


Fig. 4.13. Detail of a fracture surface in the HT 3 alloy. The alloy grains with diameters between 164 nm and 1.49 μm can be observed. LAMET laboratory.

The as-cast microstructure of the alloys in the AlCrFeNiMn system was also analyzed by optical microscopy, using the Olympus GX51 microscope, highlighting the needlelike aspect of the phases in the crystalline grains (fig. 4.14) .



Fig. 4.14. Dendritic microstructure of HT alloy 3. Optical microscopy. LAMET laboratory.

Thermal treatments were also performed to evaluate the hardening/softening effects that may occur during welding. After heat treatments, the samples were again metallographically

prepared and microhardness and microstructure analyzes were performed. The heat treatments were carried out in a Nabertherm furnace, equipped with an electronic temperature regulator, with the minimum heating rate: $0.25\text{ }^{\circ}\text{C}/\text{hour}$, 9 program memories, 4 heating ramps, 4 temperature/program interruption possibilities, programmable starting time, RS 422 interface for connecting Nabertherm MV software for control and data archiving. After the heat treatment, the samples were recut and embedded in the resin to measure the hardness (tab. 3 and 4). The thermal treatment regimes applied were:

- TT1 – furnace slow heating and maintaining for 4 hours at $700\text{ }^{\circ}\text{C}$, followed by cooling in still air (fig. 4.16);
- TT2 – furnace slow heating and maintaining for 4 hours at $700\text{ }^{\circ}\text{C}$, increasing the temperature to $1100\text{ }^{\circ}\text{C}$ and holding for 2 hours followed by cooling in still air (fig. 4.17-4.18).

After performing the TT1 heat treatment, it was found that the needlelike formations in the microstructure begin to round (fig. 4.16).

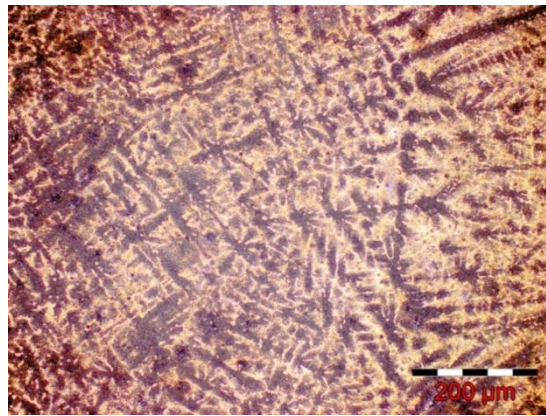


Fig. 4.16. The microstructure of the HT 3 alloy after applying the TT1 treatment. LAMET laboratory

After performing the TT2 thermal treatment, it was found that the needlelike formations in the microstructure of AlCrFeNiMn alloys tend to become more rounded, and inter-metallic compounds begin to precipitate from the supersaturated solid solution (fig. 4.17).

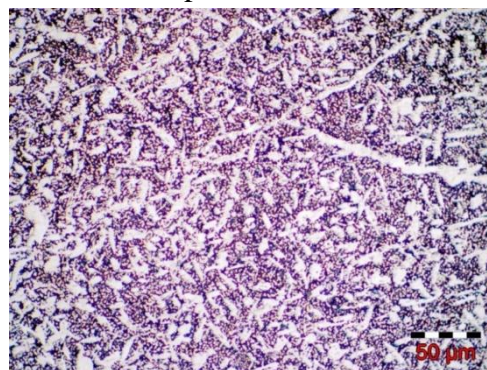


Fig. 4.17. The microstructure of the HT 3 alloy after applying the TT2 treatment. LAMET Laboratory.

At the same time, following the heat treatment, a thin layer of oxide rich in Cr and Al was formed on the surfaces, which protects the rest of the material from oxidative and corrosive effects (fig. 4.18).

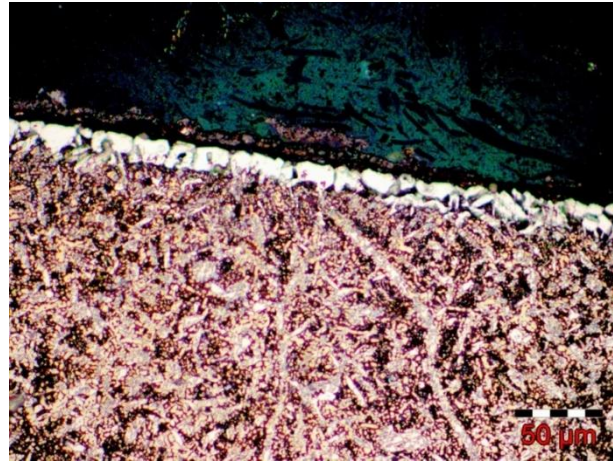


Fig. 4.18. Cross-sectional view of the edge zone of the heat-treated ingot with the TT2 regime. The formation of an oxidized layer with a thickness of about 10 μm is observed. LAMET laboratory.

The hardness of the alloys at different stages of processing was determined with the Shimadzu HMV 2T apparatus from the LAMET laboratory (fig. 4.19). The measurement conditions were: Temperature 25 ° C, Humidity 55%, pressing force 1N, pressing time 10 seconds.

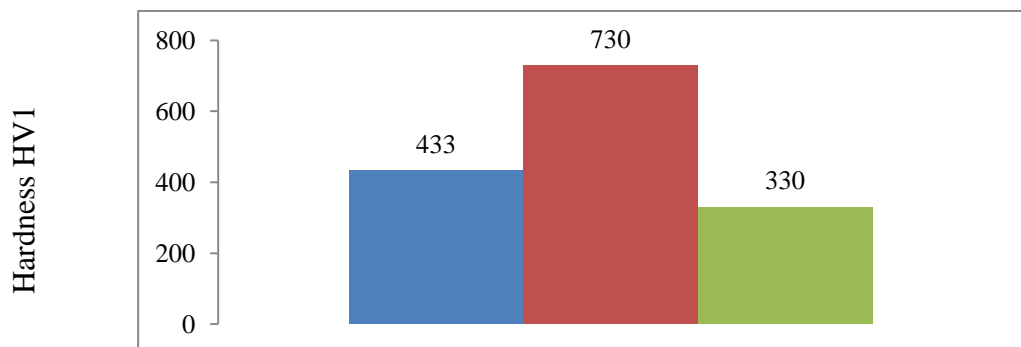


Fig. 4.19. The evolution of the hardness of the experimental alloy according to the processing state.

It is found that in the cast state the HT3 alloy has a high hardness of about 433 HV1, but after applying the TT1 heat treatment the hardness increases to 730HV1. By further applying the TT2 treatment, the hardness decreases to 330HV1. This development led to the conclusion that the HT3 alloy can be hardened after welding, if a heat treatment is applied under TT1 conditions.

4.2.2. Analysis of high entropy alloys in the AlCoCrFeNi system

$\text{Al}_x\text{CoCrFeNi}$ alloy system analysis was performed by SEM optical and electron microscopy. The HEA 1 alloy has a mole fraction of aluminum $x=1$. The value determined in the LAMET laboratory for the hardness of the experimental alloys is presented in the 4.6 chart.

Chart 4.6. HV_1 microhardness values of the as-cast HEA alloy samples

Alloy type	Exact values, HV_1	Average value
AlCoCrFeNi – HEA 1	483, 512, 509, 508, 517	500.6
Al _{0.8} CoCrFeNi – HEA 5	405, 402, 398, 415, 415	407
Al _{0.6} CoCrFeNi – HEA 6	219, 236, 214, 220, 231	224

The microstructure of the HEA 1 alloy shows dendritic formations, bordered by clearly defined grain boundaries (fig. 4.20).

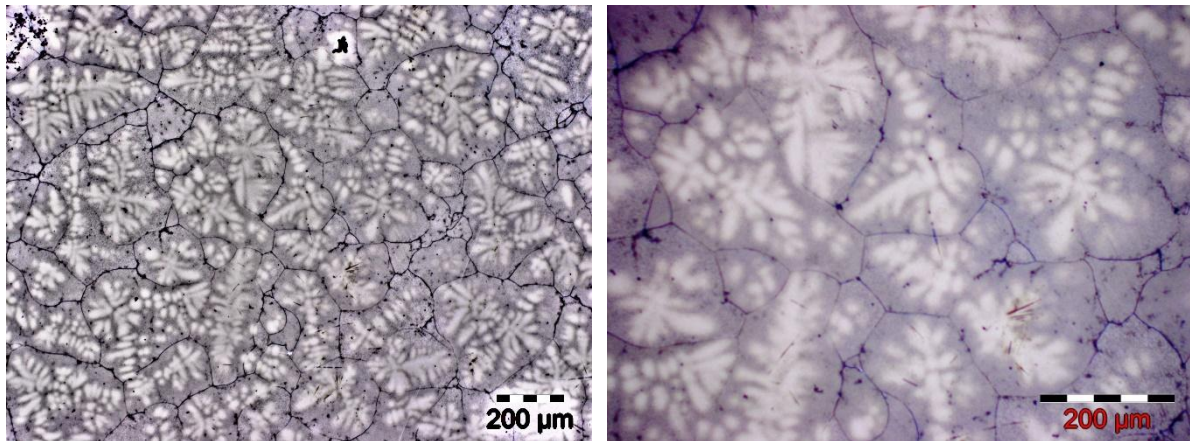
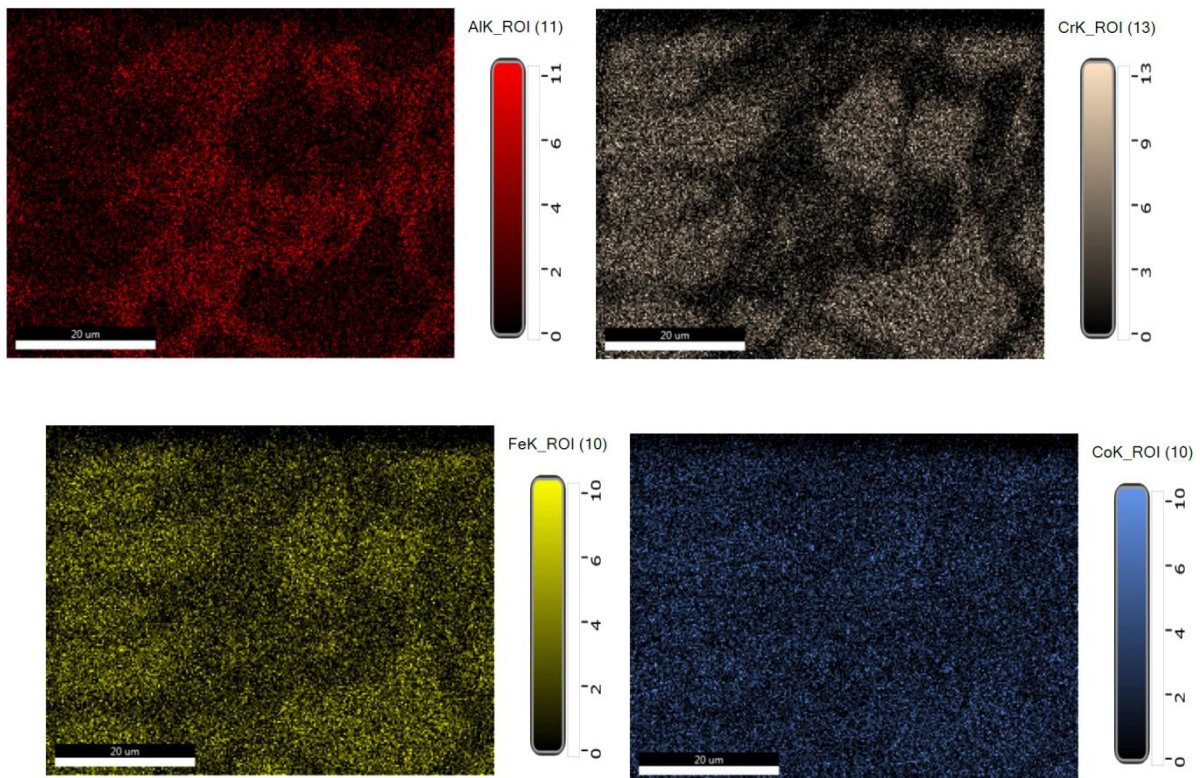


Fig. 4.20. The microstructure of the AlCoCrFeNi alloy in the casting state. Optical microscopy.

The analysis of the elemental distribution maps made with the EDAX method shows how the chemical elements are distributed and associated in the metal matrix of the HEA 6 alloy for the micro-area analyzed in fig. 4.26 (fig. 4.27).



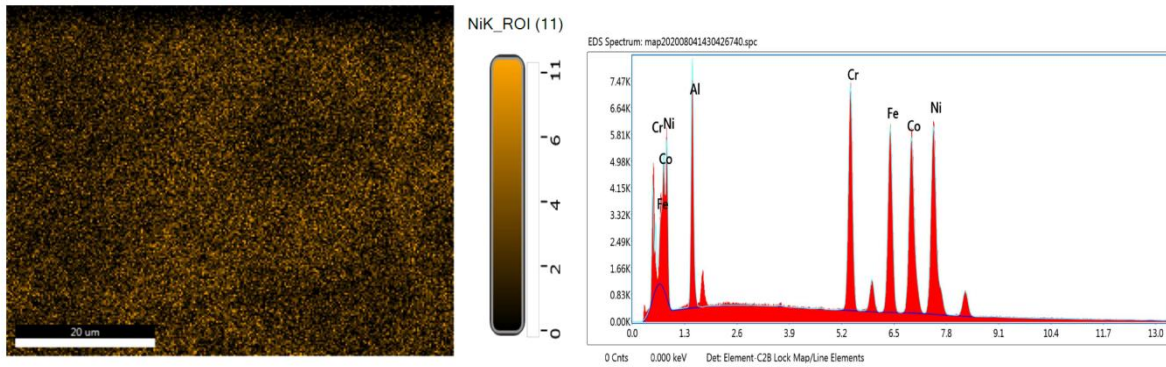


Fig. 4.27. Elemental distribution maps and chemical element spectrum for the HEA 6 alloy.

In the following writings, the effects of heat treatments on high-entropy alloys from the AlCoCrFeNi alloy system are presented. Quenching is the rapid cooling treatment of the metal alloy from temperatures in the ranges where phase transformations occur. Rapid cooling often inhibits diffusion transformations, leading to the formation of microstructures with higher hardness than the slowly cooled alloy.

To improve the mechanical properties and increase the microstructural homogeneity, the high entropy alloys HEA 6 were subjected to heat treatment cycles as follows:

- TT1, carried out for 4 hours, at 700 °C;
- TT2, performed for 4 hours, at 700 °C after which maintaining for 2 hours at 1100 °C and cooling in air (fig. 4.28).

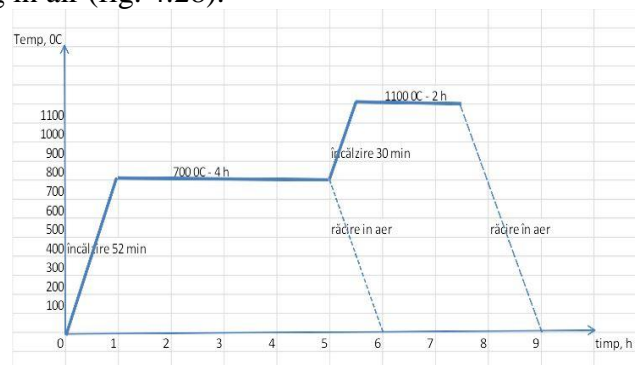


Fig. 4.28. Treatment chart applied to HEA type high entropy alloys.

4.3. CONCLUSIONS REGARDING THE OBTAINING AND CHARACTERIZATION OF THE NEW HIGH ENTROPY ALLOYS

From the heat treatment experiments it was concluded that, for alloys with high entropy, the application of successive heat treatments causes a reduction in hardness, by dissolving or putting into solution those hard compounds formed during rapid cooling during casting, which ensured the higher hardness values. In some cases, however, (e.g. HEA 6 and HT 3 alloy), the application of a single heat treatment is sufficient to obtain hardness values at an appropriate level. After the TT1 heat treatment, the average hardness of the HEA 6 alloy increased to 500 HV1 from 224 HV1 in the as-cast condition. Carrying out the second TT2 heat treatment, however, determined the reduction of hardness, to 387 HV1.

CHAPTER V. EXPERIMENTAL RESEARCH REGARDING THE RECONDITIONING BY WELDING OF WORN OUT AREAS OF THE DRILLING BITS

5.2. DESIGNING OF THE RECONDITIONING TECHNOLOGY THROUGH WELDING OF THE DRILLING BITS

For the reconditioning by welding of the worn out areas of the drilling holes the WIG (wolfram inert gas) procedure was chosen. This procedure is recommended for ferrous alloys (carbon, low-alloy, medium-alloy, high-alloy stainless steels), non-ferrous alloys of Cr, Ni, Al, Cu, Ni, Ti, in any welding position, thin components or the first layer (root) to important and intensively stressed welds from special alloys [218] .

5.2.1. Analysis of worn out surfaces for welding loading purposes

After examining the condition of the bit, it was decided to recondition it by welding, by restoring the geometry of the cones' gripping surfaces.



Fig. 5.1. Visual examination of the 3-cone drill bit and highlighting the level of wear of the ceramic elements and the areas with gripping welds of the cones.

5.2.2. Establishing the parameters of the welding regime

a) Choice of filler material

The filler materials used to perform the welds on the drill bit body were high entropy alloys, namely AlCoCrFeNi and AlCrFeNiMn. These additive materials were produced in the ERAMET laboratory in UPB, in the form of cast rods, which were then mechanically processed by turning or grinding, the obtaining process being presented in chapter IV.

5.3. RESEARCH ON THE DEPOSITION BY WIG WELDING OF HIGH ENTROPY ALLOY ADDITION MATERIALS ON STEEL TAKEN FROM THE DRILL BIT

In the first stage, depositions were carried out by welding with the WIG process, directly on the body of a decommissioned drill bit. A buffer (intermediate) layer was first deposited, over which it was loaded with high-entropy alloys from two alloying systems: AlCoCrFeNi and AlCrFeMnNi.

The main types of additive materials used in stage I of the experiments are summarized in the 5.2 Chart.

Chart 5.2. Types of additive materials for each area of the drilling bit

Welded area	Intermediate layer	Weld deposition for hard alloy loading
Zone 1	Ni-Fe base alloy wire electrode	HEA _{0.8}
Zone 2	Ni-Fe base alloy wire electrode	HT _{0.3}
Zone 3	Bohler FOX CN 22/9 N	HEA _{0.8}
Zone 4	Bohler FOX CN 22/9 N	HT _{0.3}
Zone 5	Ni-Fe base alloy wire electrode	HEA _{0.8}
	Bohler FOX CN 22/9 N	HEA _{0.8}
Zone 6	Ni-Fe base alloy wire electrode	HT _{0.3}
	Bohler FOX CN 22/9 N	HT _{0.3}



BOHLER FOX CN 22/9 N



Ni-Fe alloy rod

Fig. 5.3. Electrodes for welding the buffer (intermediate) layer.

a) Additive materials for hard loading

For the hard loading, two high entropy alloys were used, HEA0.8 and HT3 respectively (fig. 5.4). The samples were welded at room temperature without preheating.

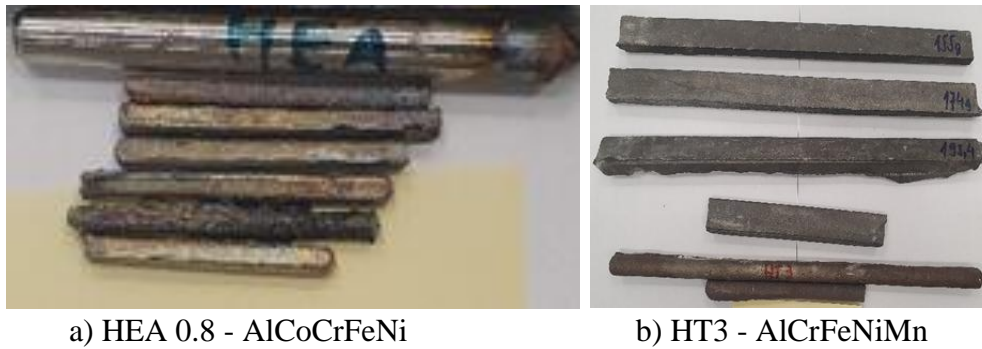


Fig. 5.4. Additive materials for hard loading by welding.

The chemical composition of the experimental alloys used for hard loading by welding is shown in the 5.3 chart.

Chart 5.3. Chemical composition of hard materials for welding

Alloy	Chemical elements, % weight				
	Al	Cr	Fe	Mn	Ni
HT3	5.73	22.08	23.78	23.35	25.06
HEA 0.8	Al	Cr	Fe	Co	Ni
	8.72	21	22.61	23.82	23.85



After welding, the samples were first examined by non-destructive methods, then cross-sections were taken for destructive tests, namely metallographic analysis, hardness levels measurements, corrosion resistance tests and wear tests.


5.4. NON-DESTRUCTIVE EXAMINATION OF WELDED SAMPLES

Within the experimental program, depositions were carried out by welding with the WIG process and high-entropy alloy filler material. Deposits were made on different areas of the drilling bit, then samples were taken for microstructure, wear, and hardness level analyzes. After complete cooling of the depositions, samples were taken from the welding loaded areas, using metal discs coated with diamond powders, under coolant liquid. The obtained samples were then subjected to processing operations with a metallographic abrasive disc under coolant liquid, to remove any heat-affected areas affected by the cutting. Analysis of the welds and testing of the submitted samples was carried out by destructive methods - microstructure, microhardness, wear resistance. For conducting the experiments, a series of samples were made, which were subsequently examined non-destructively and destructively. Since the depositions made by welding on the body of the drill bit are small in size, the number of non-destructive examination methods was restricted, the following methods being used: visual examination and penetrant liquid examination.

5.4.2. Examination with penetrant liquids

Penetrant liquid examination is a simple and easy-to-apply method for welding depositions in drill bits.

Beneficiary Polytechnic University of Bucharest Doctoral student Ștefănescu Elena	VISUAL EXAMINATION BULLETIN - WELDS Control with Penetrant Liquids – Welds deposited by TIG welding NO/NO LP DATE/DATE 12.07.2021		Code: LP-SF 02
			Page 1 of 1
			Review: 0
			LAMET Lab.
DATE DE IDENTIFICARE / IDENTIFICATION DATA			
INTERNAL ORDER / PhD Thesis Contract 06.54/01.10.2017		ASSEMBLY / Drilling bit	
IMAGE / Drilling bit 		REMARK / ITEM: SAMPLE 2 	
<i>Fig. 5.10. Area of sample 2 of the drill bit</i>		<i>Fig. 5.11. Sample 2 detail</i>	

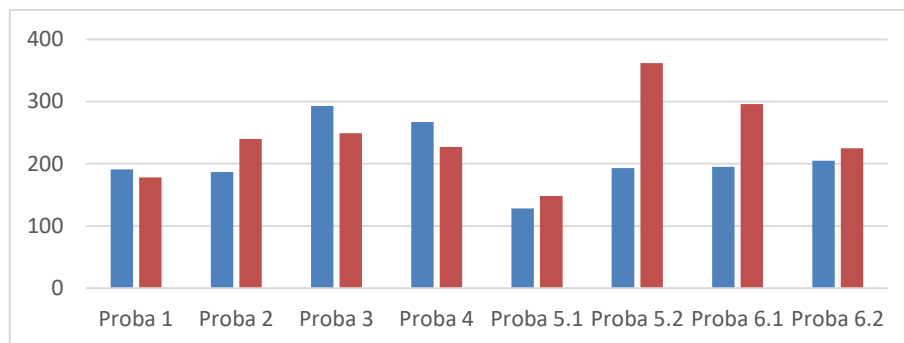
Examination technique		Examination with penetrant liquids, direct x indirect	
Examination conditions		- White light with 300lux intensity, 5x Magnifier	
Simbol și tip sudură / Weld symbol and type	Imperfecțiuni/ Imperfections *)	Rezultat / Result	Observatii / Remarks
Zone 2	 <i>Fig. 5.12. Areas with imperfections from sample 2</i>	Accepted	2017 – isolated medium pore on the central weld area

5.5. DESTRUCTIVE TESTING

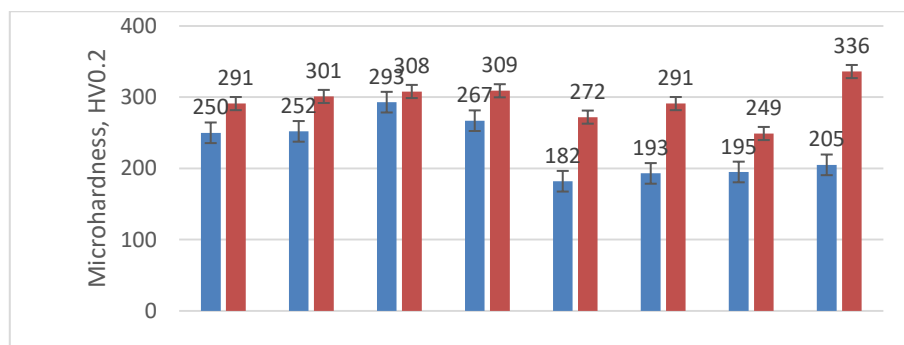
5.5.1. Hardness level measurement

For each sample made within the experimental program, microhardness measurements were performed, with imprinting in 5 different areas, after which the arithmetic average of their values was calculated. The microhardness was determined with the Shimadzu HMV 2T microhardness meter, in the LAMET Laboratory. In the study, the hardness was measured along a line that crossed the fusion line, then a minimum of 5 measurements were performed on each joint area, welded deposit respectively, fusion line, ZIT, base material.

Comparative analysis of the results obtained by measuring the hardness levels is presented in Fig. 5.25.



a)



b)

Fig. 5.25. Hardness evolution in different zones of the welded deposits.

In the heat-affected zone in the base material, hardness values between 249 -308 HV were measured. The increase in hardness levels in this zone was due to both the quenching effect of rapid cooling after welding and the enrichment with alloying elements diffused from the weld deposit.

From Fig. 5.25a it is observed that the highest hardness value was obtained in the case of sample 5.2 and sample 6.1, where a high alloy austenitic stainless electrode was used as a buffer layer.

In samples 1, 3, 4 the hardness level was higher on the base material. This was due to the fact that the buffer layer, made with a soft nickel alloy, caused a dilution of the metal deposited by welding with the HEA alloy. In conclusion, the combination between the HEA0.8 hard alloy with a buffer layer deposited with the Bohler FOX CN 22/9 N stainless electrode (sample 5) and

the HT 3 hard alloy with a buffer layer also from the Bohler FOX stainless electrode CN 22/9 N (sample 6) was determined as the optimal charging material.

From Fig. 5.25b it is observed that in all cases the hardness in the thermo-mechanically influenced zone (ZIT) is higher compared to the base material, the biggest difference being recorded in the case of sample 6.2. Hardening in ZIT occurs as a result of rapid cooling after loading by welding and the formation of hard, martensite-type phases in the microstructure. Hardness values between 199-296 HV were recorded on the fusion line, comparable to those in ZIT. These values correspond to a ferritic-austenitic steel containing additional Al and Co elements.

The scanning electron microscope SEM/EDAX Quanta Inspect S, Q47 (fig. 5.26) was used for the analysis of the appearance of the welded areas and the determination of the chemical compositions on micro-areas (SEM and EDX analyzes).

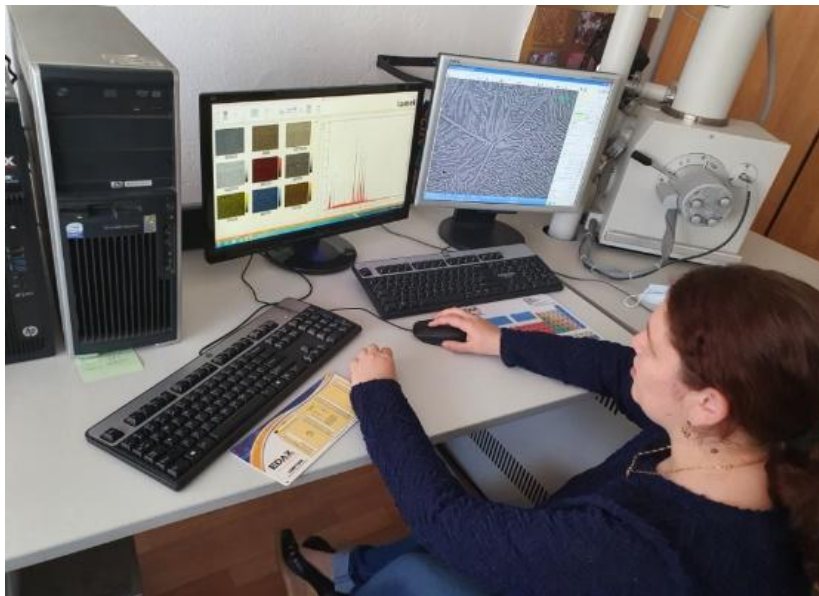
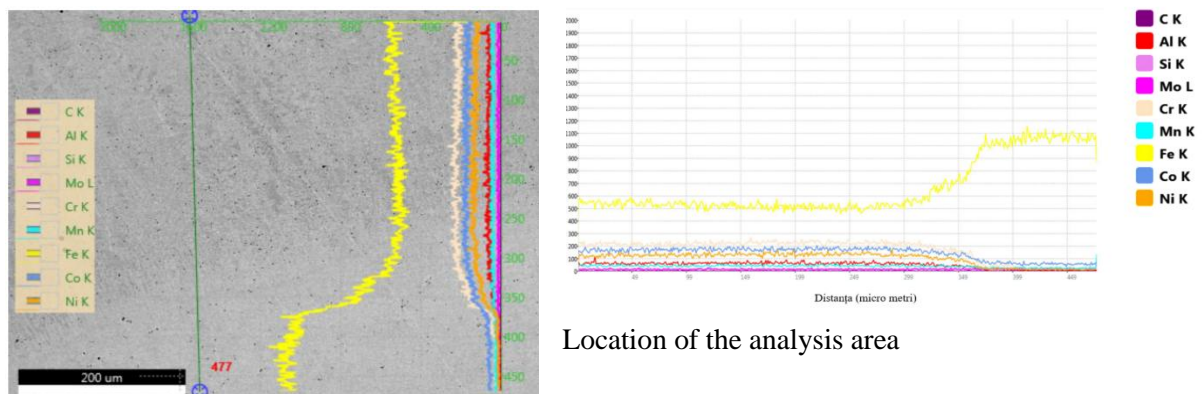


Fig. 5.26. Scanning electron microscope SEM Inspect S, Q 47, equipped with EDAX Ametec 2E analyzer, LAMET Laboratory.

In order to estimate the effects of the diffusion of chemical elements between the welded deposit and the manganese steel substrate (from which the body of the drill bit is made), an EDAX analysis was performed along the length of a line that crossed the separation line between the weld and the base material (Fig. 5.27).

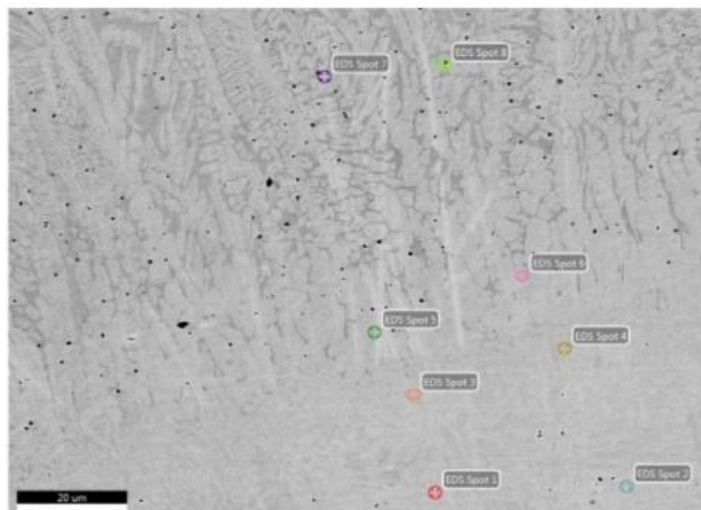


Location of the analysis area

Distribution lines of the chemical compounds for the main chemical elements in the welded joint corresponding to sample 5.2.

The quantitative measurement of the chemical composition was carried out in different areas of the cross section of sample 5.2 (Fig. 5.28), as follows:

- Points 7 and 8 – located in the weld
- Points 5 and 6 - on the weld separation interface from the base material
- Points 3 and 4 - in the ZIT, close to the weld interface
- Points 1 and 2 - in ZIT at a distance of about 20 microns from the weld interface



a) Location of chemical compound measurement areas

Chart 5.14. The actual values of the chemical compound in point 7

Element	Weight %	Atomic %	Net	Error
C	0.79	3.38	3.96	18.33
Al	5.75	10.90	117.35	9.38
Si	0.61	1.11	17.42	13.12
Cr	14.73	14.48	469.31	2.27
Mn	0.49	0.46	14.07	18.41
Fe	47.55	43.54	1154.70	1.90
Co	15.38	13.34	326.26	2.43
Ni	14.69	12.79	273.32	3.15

As it follows from the chemical compound values presented in the 5.14 chart, at a distance of approximately 60 μm from the fusion line, the concentration of the main chemical elements in the welded deposit contains, in addition to Fe, both elements from the electrode used to make the buffer layer (14.7 % Cr, 14.69 % Ni) as well as from the high entropy alloy bar (5.75% Al, 15.38% Co). It can be said that, during welding, a new high-entropy alloy was created "*in-situ*", resulting from the rapid mixing of the two filler metals.

Elemental distribution maps for the microzone analyzed from the welded joint in the case of sample 5.2. are shown in Fig. 5.36.

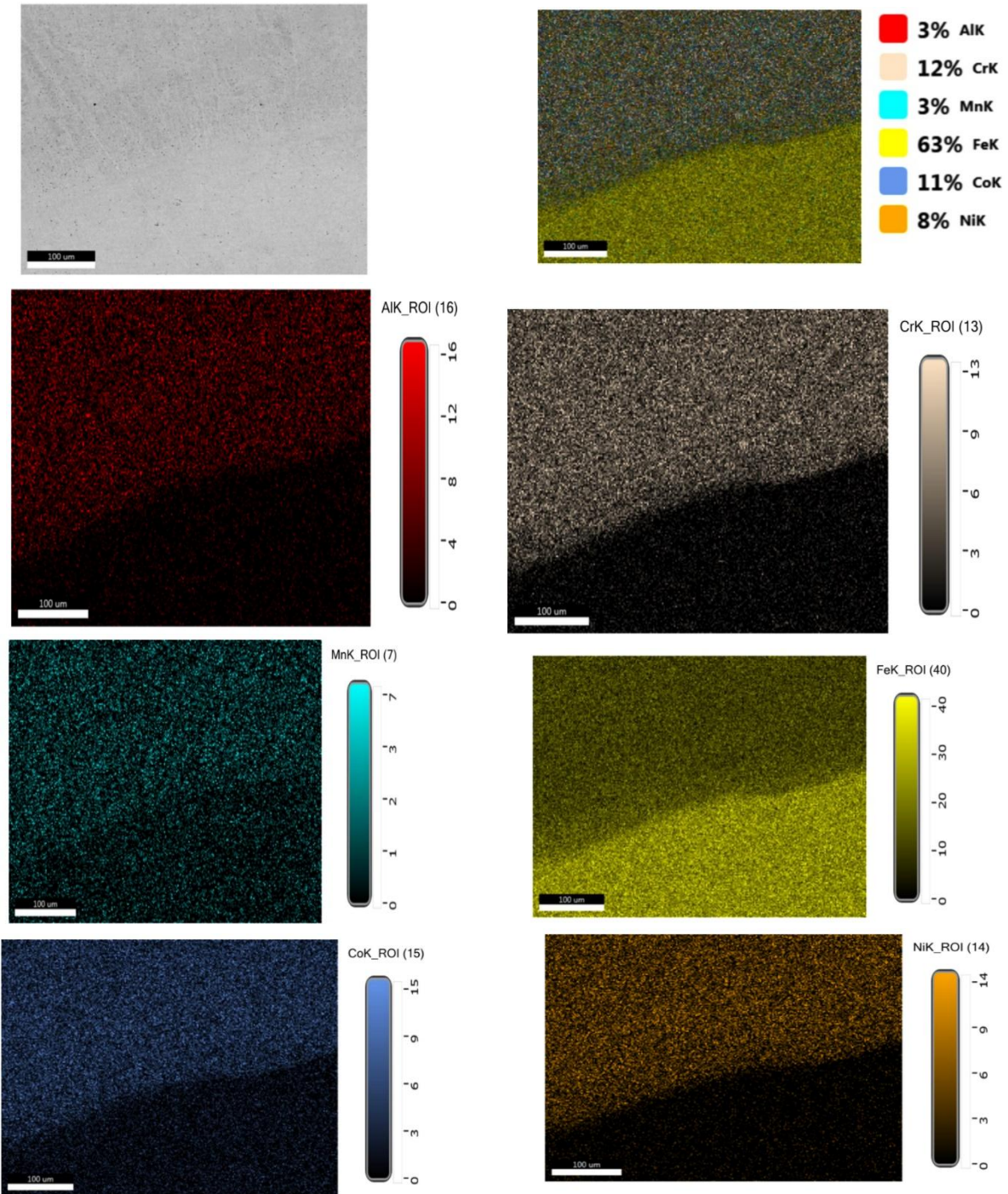


Fig. 5.36. Elemental distribution maps for sample 5. LAMET Laboratory.

From the distribution of chemical elements shown in Fig. 5.36 it can be seen that the main alloying elements (Cr, Co, Al, Ni) are uniformly distributed in the welded deposit. At the same time, it can be observed that elements such as Cr, Ni, Al, Co predominate in the welded deposition, while Fe is the majority element in the base material, located at the base of the figures.

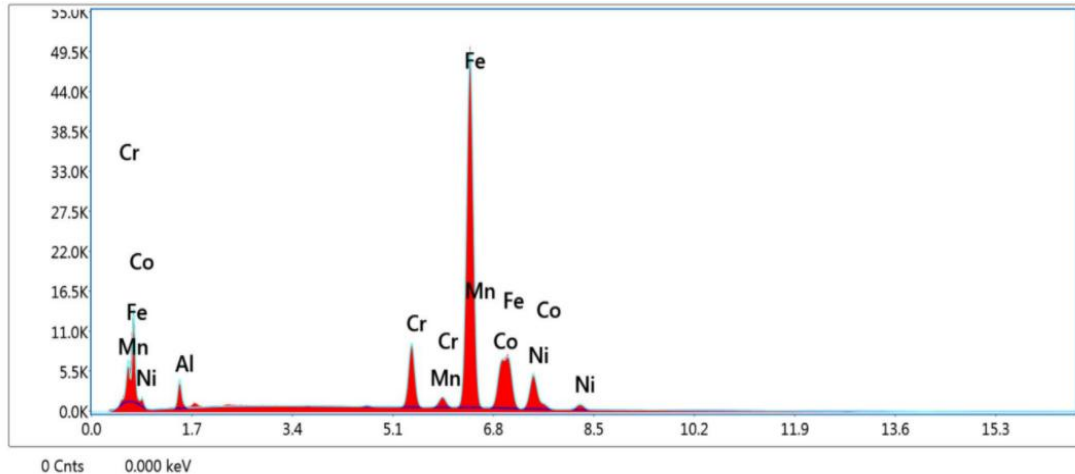


Fig. 5.37. The global spectrum of the chemical elements in the microzone analyzed in fig. 5.34.

In order to highlight the microstructural aspects by examining with an optical microscope, the samples were subjected to an attack with the chemical reagent Nital 2%, after which they were washed with water and dried with hot air. The analyzes were performed on cross-sections taken from the samples loaded by welding on the drilling bit.

All microscopy examinations were carried out at a temperature of 24 °C and a humidity of 54%, according to the LAMET Laboratory Measurement Procedure (UPB - PO - 05.03.02, SR EN ISO 17639: 2014 and SR CR 12361 + AC: 1999) (Fig. 5.38).

Images of the optical microstructures of the samples welded on the drilling bit and their interpretations are presented in Fig. 5.39.

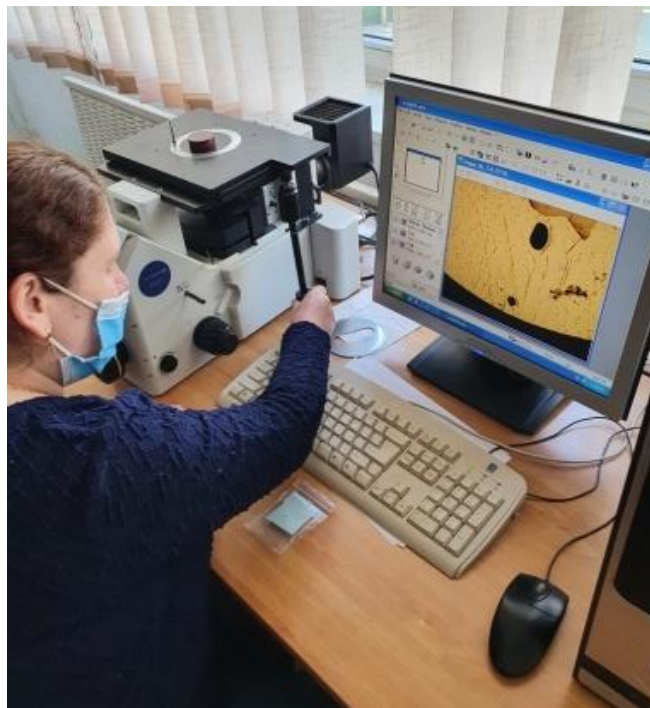
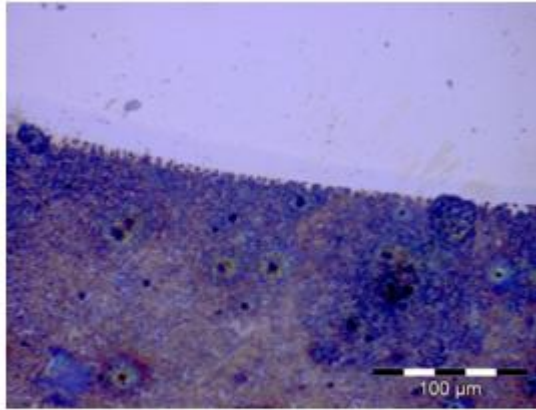
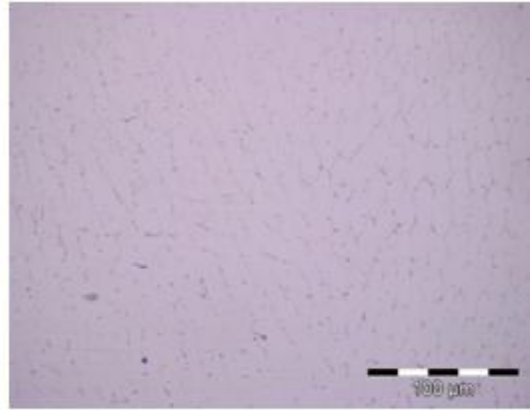


Fig. 5.38. Performing analyzes with the Olympus GX51 metallographic microscope, LAMET Laboratory.

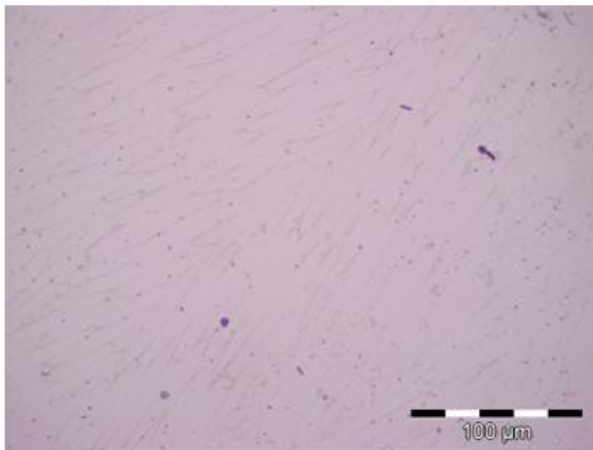


Microstructură MB-sudura, P1 (mărire 500X)

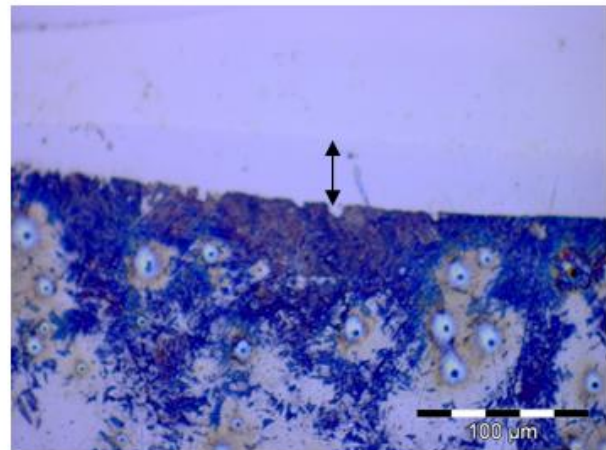


Microstructură sudura, P1 (mărire 500X)

The weld shows a dendritic microstructure with small precipitations of inter-metallic compounds and the base material has a microstructure of needlelike pearlite and nodular inclusions. The fusion line, which represents the interface between the base material and the welded deposit, is continuous, without imperfections. An interpenetration effect of the deposited metal towards the base metal can be observed.



Microstructură sudură, P5.1 (mărire 500X)



Microstructură ZIT, P5.1 (mărire 500X)

The buffer layer area is delimited by the arrow. The microstructure of the weld is dendritic, without imperfections. The base material (located at the base of the image) reacted and colored more strongly than the weld.

Fig. 5.39. Metallographic analyzes of samples with welded deposits made on the drilling bit, batch I.

5.6. PERFORMING EXPERIMENTS OF DEPOSITION OF HARD LAYERS WITH HIGH ENTROPY ALLOYS ON THE DRILLING BIT. THE SECOND BATCH

After making and identifying the HEA alloy with the best hardness level and wear resistance characteristics, we moved on to a second set of welding experiments. The same TIG welding process and SAF-FRO power source were used. To carry out the tests, flat portions were cut from the bit jaws, which were mechanically processed by milling, then cleaned with ethyl alcohol and dried, to be prepared for welding (fig. 5.40).



Fig. 5.40. Samples taken from the drilling bit to be loaded by welding.

Layers of high-entropy alloys (HT3, with the chemical compound, weight %: Al = 4.72; Cr = 26.44; Mn = 22.56; Fe = 25.82; Ni = 20.46) were deposited on the flat surfaces of the samples, without a buffer layer. The loading by welding was carried out with the WIG process, with the same values of the welding regime parameters as the samples from the first batch. After the loading by welding, the samples were divided in two parts, one of the samples being intended for metallographic analyzes in the welded state, and the other half from each sample was subjected to thermal treatments (fig. 5.41).



Fig. 5.41. Cross-sections through the samples loaded by welding with the HEA 6 alloy.

The thermal treatment applied to the samples loaded by welding on the drilling bit was carried out with the Nabertherm furnace, and the thermal regime was:

- | | | | |
|------------|--|------------|--|
| TT1 | - heating with the furnace up to 700 °C; | TT2 | - heating with the furnace up to 700 °C; |
| | - maintaining at the same temperature level for 4 hours; | | - maintaining at the same temperature level for 4 hours; |
| | - furnace cooling. | | - cooling in water (quenching). |

After performing the thermal treatments, the samples were again subjected to hardness level tests, the results being presented in the 5.18 chart.

Chart 5.17. HV₁ microhardness level values of the welded and heat-treated samples

Alloy type	Exact values, HV ₁	Average value, HV1
SUDURA	412, 388, 408, 386, 418, 432, 387, 352, 528, 445	416
S1-SUD+TT1	370, 430, 397, 492, 405, 365, 437, 352, 357, 357	396
S2-SUD+TT2	482, 455, 481, 487, 539, 497, 520, 547, 524, 563	510
MB	249, 240, 252, 269, 240, 269, 254, 248, 248, 261	253
MB+TT1	194, 194, 185, 181, 178, 186, 188, 176, 171, 193	185
MB+TT2	372, 376, 353, 356, 376, 493, 359, 460, 345, 379	380

From the results presented in the 5.17 chart it can be seen that the deposition made by welding with HT3 alloy has a higher hardness than the base material (MB), by about 163HV1. By applying the quenching heat treatment T1, which is a homogenization annealing, the hardness decreased in both the weld (396 HV1) and the base material (185 HV1).

The value was also determined of the roughness levels of the metallographically processed surfaces with the Vogel Germany digital roughness meter (5.18 chart), these being subsequently subjected to wear resistance tests.

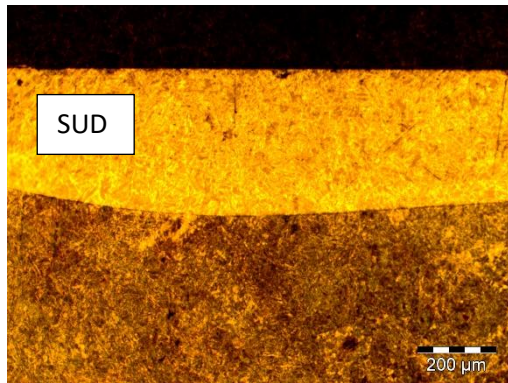
Chart 5.18. The roughness level values of the samples taken from the drilling bit

Alloy type	Roughness, R _a μm	Average value
S ₁ SUD	0.082, 0.088, 0.094, 0.081, 0.085	0.086
S ₁ TT1	0.166, 0.308, 0.152, 0.13, 0.152,	0.181
S ₂ SUD	0.036, 0.034, 0.036, 0.034, 0.039	0.0358
S ₂ TT2	0.037, 0.031, 0.03, 0.034, 0.027	0.0318
MB	0.029, 0.031, 0.038, 0.031, 0.033	0.0324
MB TT	0.036, 0.034, 0.042, 0.029, 0.036	0.0354

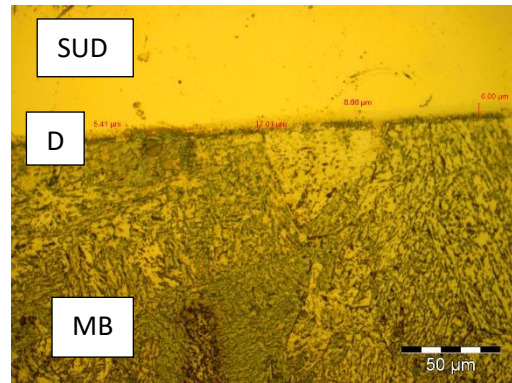
5.7. METALLOGRAPHIC ANALYSIS OF TIG WELD DEPOSITS USING HIGH ENTROPY ALLOYS FROM THE AlCrNiFeMn ALLOY SYSTEM

a) Analysis by optical microscopy

The samples were subjected to the metallographic preparation procedure, which consisted of grinding using abrasive papers with progressive grit (from 360 grit to 2500 grit), then polishing with fine alumina powders, with grit from 3 μm to 0.1 μm. After polishing, the samples were washed with ethanol, then attacked with 2% Nital chemical reagent. The Nital reagent was used to highlight the microstructure of the base material (of the drill bit), which is a steel alloyed with Mn. The optical microscopy images taken with the Olympus GX51 microscope are shown in figure 5.43.



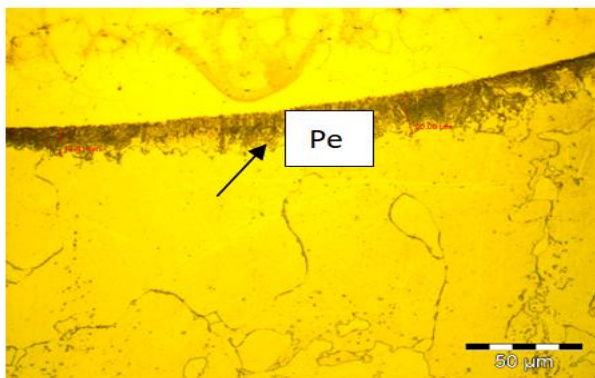
Cross-sectional view of the deposition made by welding with HT 3 alloy. The continuity and good adhesion of the welded deposit, (SUD), without imperfections can be observed. 100x magnification



Detail of the transition zone between the welded deposit (SUD) and the base material (MB). A dilution zone (D) between 5 and 8 μm thick can be observed. 500x magnification

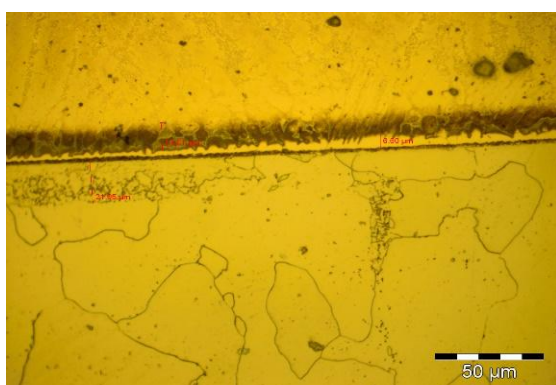
Fig. 5.43 . Appearance of the transition zone between the base material and the welded deposit with HEA6 alloy.

The welded samples were then subjected to thermal treatments (TT1 and TT2), the optical microscopy images being shown in fig. 5.45.

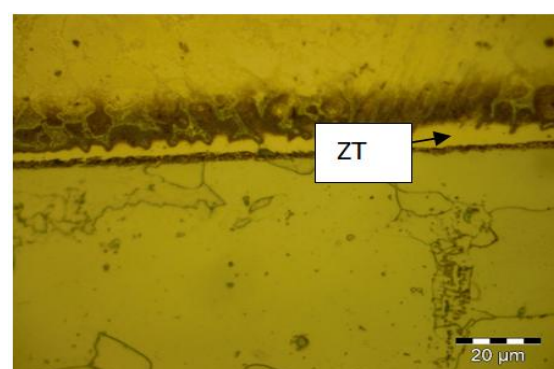


A narrow zone is observed near the fusion line (about 20 μm thick) in which there is still undissolved pearlite.

Fig. 5.45 . The ZIT of S1-TT1 sample.



500x magnification



1000x magnification

Fig. 5.46 . The ZIT of S2-TT2 sample. Details on the area adjacent to the fusion line. Spheroidized carbides are observed located in the ferrite grains or accumulated towards the fusion line, on an area of about 21 μm. On the other side of the fusion line, in the weld, a transition zone was formed, with a width of about 6 μm

a) Analysis by scanning electron microscopy (SEM) and chemical microcomposition/energy-dispersive X-ray analysis (EDAX)

The high entropy alloy used as filler material in this set of experiments was selected from the AlCrFeNiMn alloy class to further reduce manufacturing costs by removing Co from the product recipe and replacing it with Mn. The chemical microcomposition analysis of the used alloy was carried out by X-ray spectrometry, with the EDAX method (fig. 5.47).

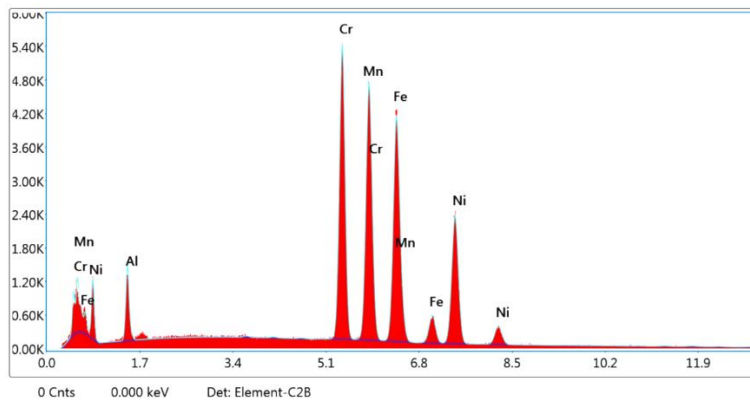
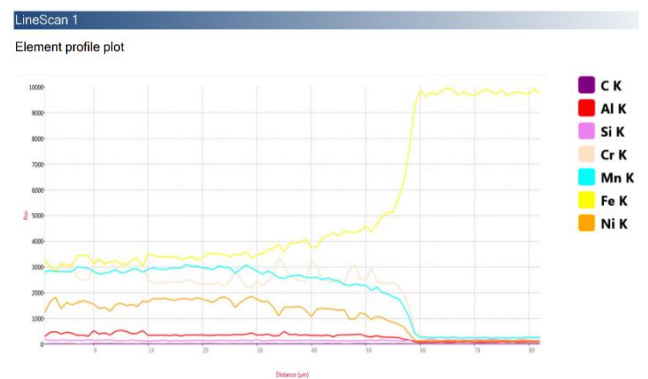
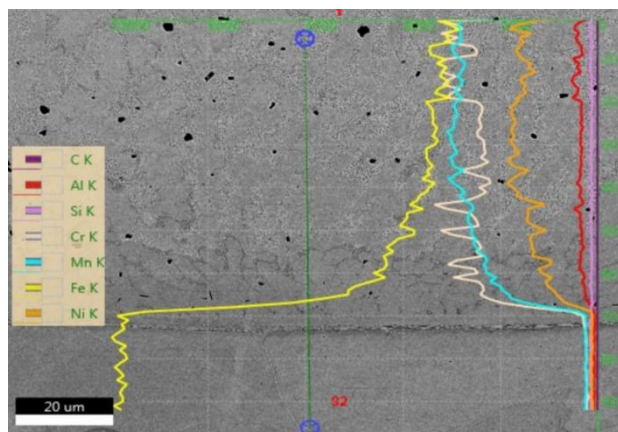


Fig. 5.47 . Result of chemical compound analysis by EDAX method for high entropy alloy filler material

We then went on to observe each zone of the welding deposition, being analyzed in detail especially the welded deposition and the transition zone to the base material, which is the center of the diffusion phenomena (fig. 5.48). In the image in Fig. 5.48 we can observe distribution lines of chemical elements in the S2 TT sample, which record a sudden decrease in the concentration for Cr, Ni, Mn when approaching the fusion line (fig. 5.48a), over a distance of approximately 10 μm , which corresponds to the non-mixing zone identified in the optical microscopy analysis (fig. 5.48b). At the same time, a proportional increase in Fe, the major element in the drill bit steel, is observed.



b)

a)

Fig. 5.48 . S2 TT Sample. Representation of chemical element distribution along a 92 μm line crossing the transition zone between the weld deposit and the base material (drill bit steel).

SEM microscopy analysis of the ZIT (fig. 5.49) revealed, at a 5000x magnification (fig. 5.49b), the formation on the fusion line (LF) of a transition zone between the two alloys, where the chemical elements from highly alloyed weld deposits have a tendency to diffuse rapidly, especially on the boundary between the ferrite grains of the drill bit steel (red arrow).

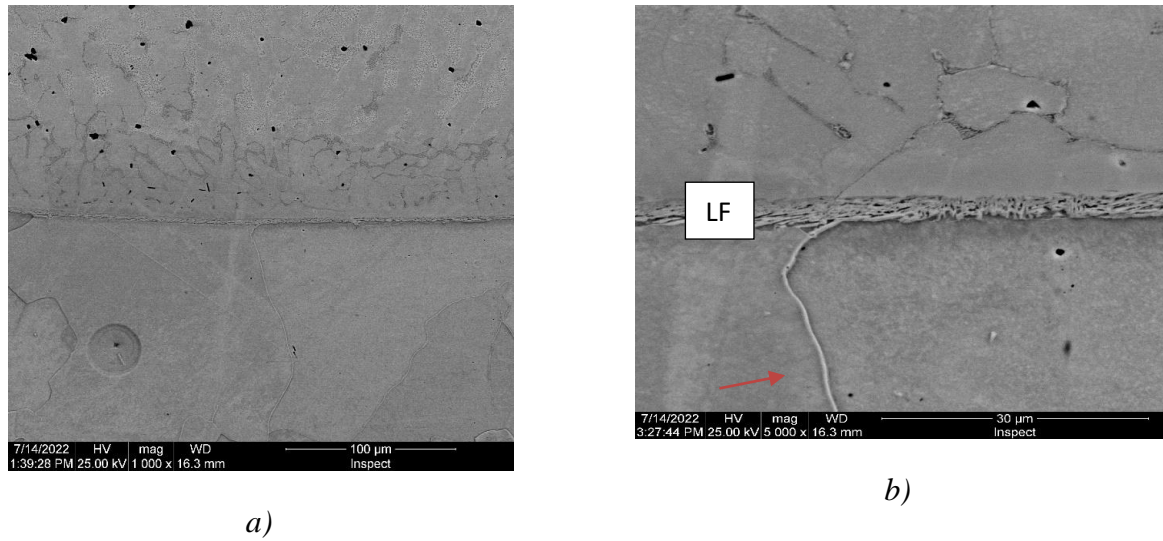


Fig. 5.49 . Analysis of the fusion line between the weld deposit and the base material. S2 TT Sample.

For the detailed analysis of the welded deposition, elemental distribution maps (fig. 5.58) and spot analyzes of chemical micro-compound (fig. 5.59) were carried out, which highlighted the in-situ formation of Al-N type *compounds*. The results of the chemical micro-compound analyzes in fig. 5.56 are shown in fig. 5.60 – 5.63

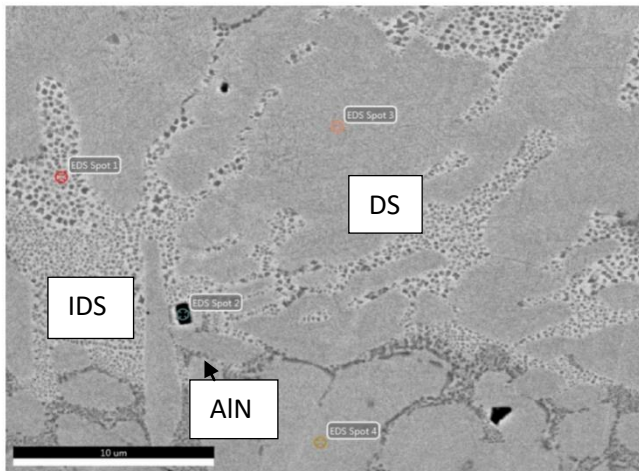
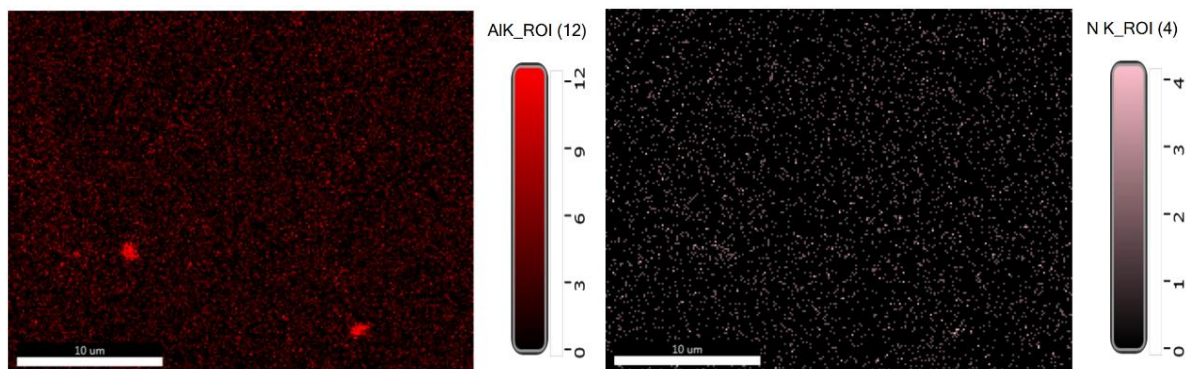


Fig. 5.58. Location of points of analysis of the micro-chemical compound of the welded deposit. S2TT sample.

Very compact dendritic areas (DS) and interdendritic areas (IDS) can be observed, in which the presence of some compounds is noted. At the same time, dark colored polyhedral compounds (AlN) can be observed.



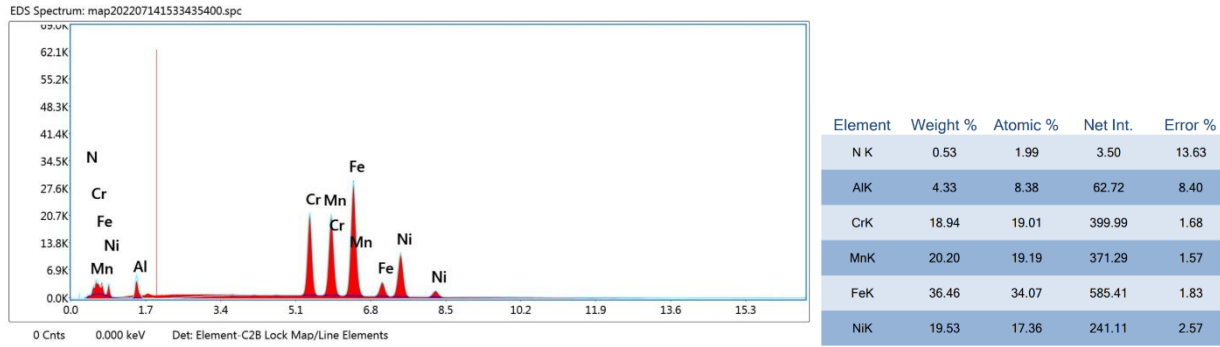


Fig. 5.59. Elemental distribution maps for Al and N and quantitative EDAX analysis of the micro-area in fig. 5.58.

To compare the effects determined by the heat treatment, similar analyzes were performed on the S1TT sample, which was heat treated by annealing at 700 °C for 4 hours and slow cooling via the furnace.

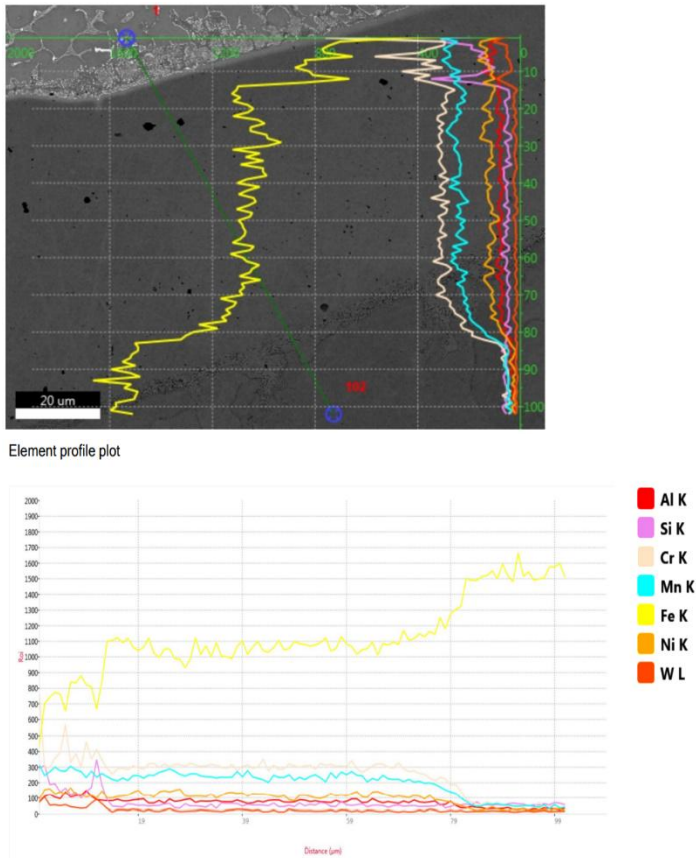


Fig. 5.64. S1 TT Sample. Distribution of chemical elements along a 102 μm line crossing the transition zone between the weld deposit and the base material (drill bit steel).

The transition zone (ZT) was identified only in the welded S1 TT sample, in which the effect of the slow cooling annealing heat treatment was manifested by the reduction of the hardness levels and the formation of a diffusion band of chemical elements, on a width of at least 80 μm. The width of this zone varies in different portions of the root of the welded deposit, the largest being right there. At the same time, it was noted, in this sample, a type of non-conformity

that appeared only in the welded deposition, namely massive inclusions of W, originating from the impurities from the molten drops detached from the tip of the non-fusible W electrode used for welding.

In the central area of the deposition, as a result of the very high density of W (19.30 g/cm^3), accumulations with this element (red areas) were formed, located immediately next to the fusion line (fig. 5.64), which distorted its linearity. At the same time, accumulations of silicon (purple colored areas) and aluminium (deep red) can be observed, while Cr, Ni and Mn are located on areas with an inter-dendritic appearance.

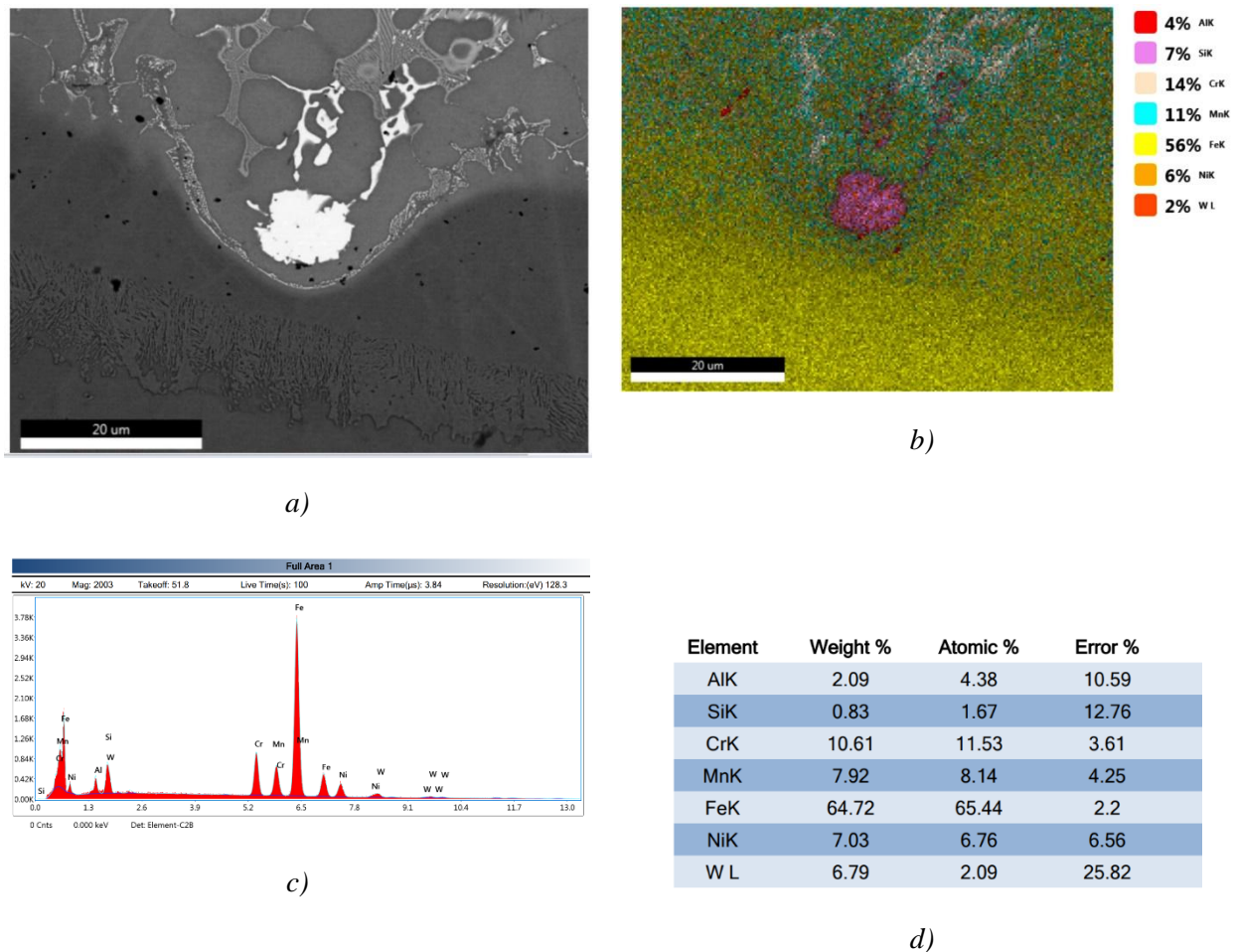


Fig. 5.66. Central area of the deposit with W and Si inclusions located at the fusion line of the welded deposit in the case of the S1 TT sample. a) SEM image; b) distribution map of the main chemical elements; c) the spectra of the main chemical elements identified on the selected micro-area; d) concentration values of chemical elements.

In the case of the S1 TT sample, from the analysis of the results obtained by the local chemical compound measurements performed on phases in the transition zone between the welded deposit, the transition zone and the base material of the drilling bit, the following observations result:

- A significant impurity of the W welding deposition was identified from the partial melting of the tip of the electrode used in TIG welding, either due to the poor quality of the electrode or due to its overheating during welding; thus, concentrations between 7.58

and 15 wt% W were measured in the welded deposit, 9.28-9.91 wt% respectively at the level of the fusion line;

- Immediately below the fusion line of the welded deposit, a transition zone was identified, with a width between 80 and 100 μm , in which the effects of the diffusion of chemical elements from the welded deposit to the steel substrate of the drill bit were manifested [220];

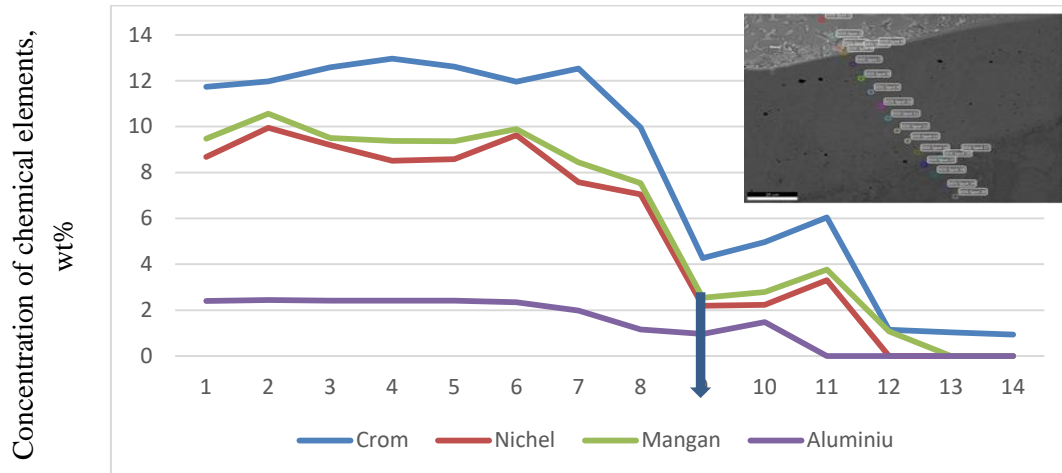


Fig. 5.87. Evolution of the concentration of the Cr, Ni, Mn, Al elements in the transition zone, from the fusion line to the base material

From Fig. 5.85 it can be seen how the concentration of the main chemical elements (Cr, Ni, Mn, Al) in the transition zone begins to decrease as it approaches the separation line with the base material of the drilling bit (point 9 of the diagram in fig. 5.85). At a distance of about 20 μm from the fusion line, the lowest values of the alloying elements are recorded. The element with the greatest diffusion tendency is also in this case Cr. It has a concentration of 6wt% at the fusion line and about 1wt% at a distance of 20 μm from it. All other main chemical elements (Ni, Mn, Al) no longer diffused significantly below the fusion line.


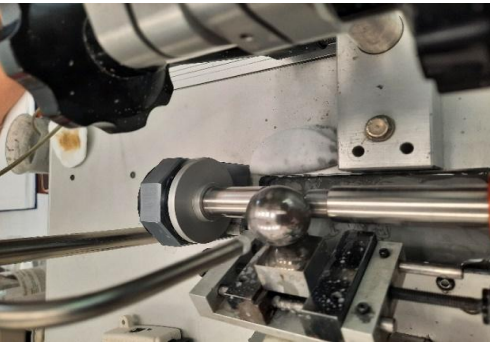
5.8. CONCLUSIONS REGARDING THE WELD DEPOSITION BEHAVIOR OF HIGH ENTROPY ALLOYS ON DRILLING BITS

- The high-entropy alloys used for the reconditioning of the drill bits had a suitable behavior when welding, following the control with penetrant liquids, no crack-type imperfections were identified.
- The use of a buffer layer to reduce the diffusion effect of the alloying elements from the hard deposit to the manganese steel substrate resulted in a reduction in the hardness levels of the deposited layer.
- Elemental distribution analyzes on a line crossing the weld-to-drill bit metal interface revealed that there are no significant diffusion effects of elements from the hard deposit to the substrate, which is explained by the slow diffusion effect specific to high entropy alloys. This demonstrates that a buffer layer is not necessary for this application.
- The results obtained from the hardness test showed an increase in the hardness of the high entropy alloy weld deposit to a maximum of 416 HV1, compared to the drill bit base material of 253 HV1.
- The application of an annealing heat treatment after welding, carried out at 700 °C, followed by water cooling, resulted in an increase in hardness to about 510 HV1, which allows an increase in wear resistance on the loaded areas.

CHAPTER VI. TESTING OF WELDING LOADED SAMPLES

6.1. TRIBOLOGICAL ABRASION TESTS PERFORMED FOR DEPOSITS WELDED WITH HIGH ENTROPY ALLOYS

The test to determine the wear resistance of high entropy alloys deposited layers aimed to estimate the behavior of the new materials under simulated conditions similar to those during drilling. For this purpose, the samples taken from the welding loaded areas, were processed to similar roughness values, $R_a = 0.220 - 0.287 \mu\text{m}$. To simulate wet wear conditions, an abrasive solution of SiC in water suspension was injected between the test piece and the pressing ball of the device, with a constant flow ensured by the CALOWEAR CSEM device (Fig. 6.1 and 6.2).

The method used	DEVICES
<p>During the tribological test, the hard steel ball was pressed against the surface loaded by high entropy alloy welding, applying a desired value of pressing force. Then the diameter of the wear crater was measured (by optical microscopy) and based on the measured values, calculations were made to estimate the wear resistance. The ball performs a rotational movement because it is driven by means of a shaft connected to an electric motor, for which the desired speed can be adjusted (Fig. 6.2). By rotating, the ball drives the abrasive particles from the continuously dispersed solution into the working space and presses it against the surface of the part with a known force, thus generating a wear imprint.</p> <p>The parameters of the test regime were:</p> <ul style="list-style-type: none"> - Ball diameter: $d=25.4$ [mm] - Ball material: bearing steel, hardened - Pressing force: F_N [N] - Number of revolutions at the drive shaft: n - Test time: t[s] <p>Abrasive solution type</p>	 <p><i>Fig. 6.1. Overview of the CALOWEAR CSEM device</i></p>  <p><i>Fig. 6.2. Detail on the testing area</i></p> <p>SiC, particles with an average diameter of $4.5 \mu\text{m}$ in a distilled water suspension with a concentration of 50 ml SiC/173 ml H₂O.</p>

Results and discussions

The CSEM Calowear machine is an instrument that performs small-scale abrasive wear tests. It allows the evaluation of the intrinsic wear coefficient for material surfaces or for certain substrates, as well as for their various deposits. For each sample, 2 abrasive wear tests were performed, after which the diameter of the footprint resulting from the friction between the test ball and the surface of the sample was measured, between which the abrasive fluid was continuously injected. (Fig. 6.3a).

The surfaces of the samples were polished with abrasive papers under identical conditions, the roughness value determined with the Vogel digital roughness meter, Germany, being between $R_a = 0.222 - 0.287 \mu\text{m}$ (Fig. 6.3b and 6.3c). The measurement of the diameter of the footprints was made with the Olympus GX51 microscope, equipped with the image analysis and measurement program, AnalySIS (Fig. 6.4).

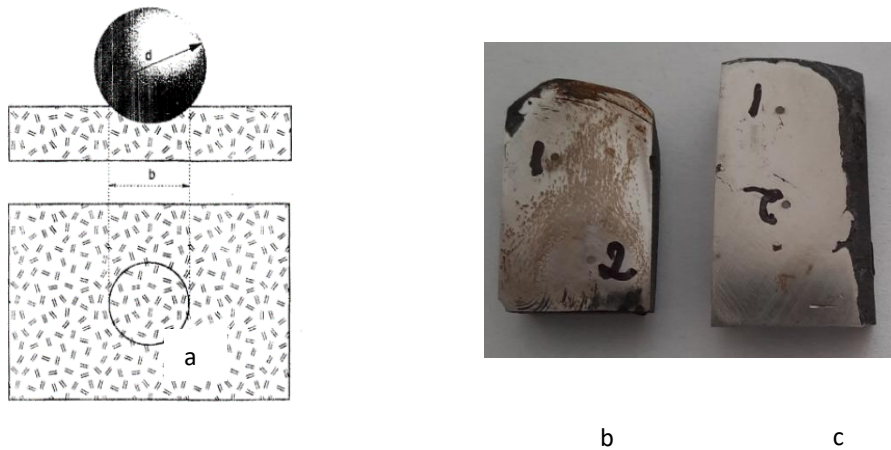


Fig. 6.3. The principle of the Calowear method (a) and how to prepare samples from the 1 SUD batch for the wear test (b) 1 SUD sample and (c) 1 TT sample. It is noted that the surface has been polished with sandpaper and the wear marks are spaced and numbered 1 and 2.

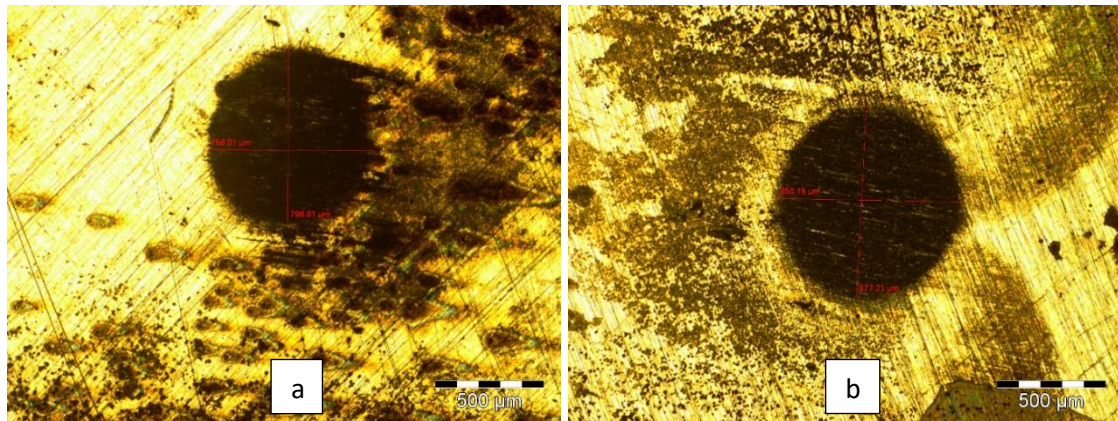
The values of the footprints' diameters were used to perform the calculations of the wear resistance parameters which are presented synthetically in the 6.1 – 6.6 charts.

The smaller the value of the diameter of the wear footprint, the higher the wear resistance of the material.

Chart 6.1. Wear test results for Sample 1 SUD

No. Crt.	Testing time [s]	Friction length [mm]	Loading force F_N [N]	The wear coefficient k [mm^3/Nm]	The volume of worn out material [mm^3]	The wear intensity,	Depth, [mm]
1	900	214956.28	0.28	2.09771E-08	0.001262564	2.617E-08	0.005625354
2	900	214956.28	0.37	2.53682E-08	0.002017632	3.3082E-08	0.00711122

1 SUD and 1 TT samples were taken from the same welding deposition, performed with the same filler material. 1SUD sample is in a welded condition and 1 TT sample is welded and then heat treated.

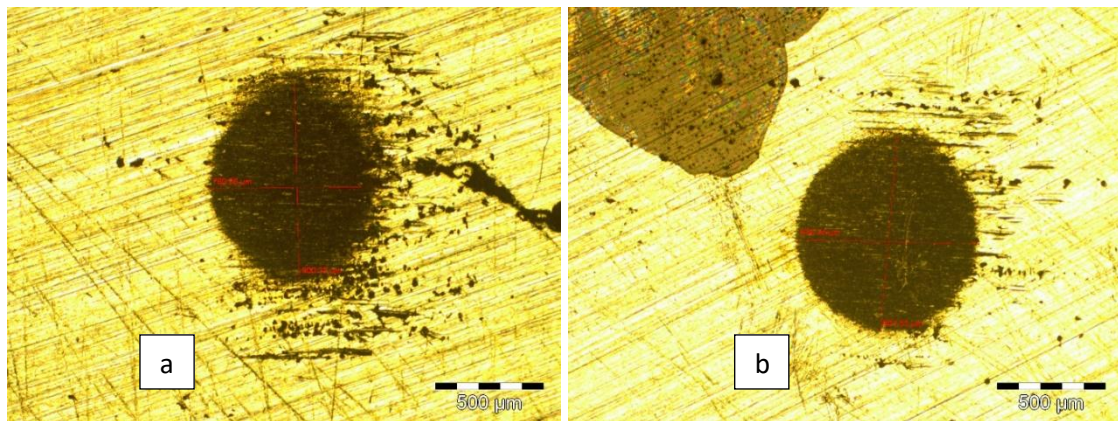


A1 Footprint *A2 Footprint*
 Fig. 6.4. Diameter measurement of wear marks for 1SUD sample (μm)

Diameter along the 1 direction, μm	Diameter along the 2 direction, μm
756.01	850.15
796.01	877.21

Chart 6.2. Wear test results for 1 SUD TT Sample

No. Crt.	Time [s]	Friction length [mm]	Loading force F_N [N]	The wear coefficient k [mm^3/Nm]	The volume of worn out material [mm^3]	The wear intensity,	Depth, mm
1	900	214956.28	0.308	2.16095E-08	0.001430687	2.7858E-08	0.005988189
2	900	214956.28	0.306	2.87025E-08	0.001887953	3.2001E-08	0.006878898



A1 A2
 Fig. 6.5 Diameter measurement of wear marks for the 1 SUD TT sample (μm)

Diameter along the 1 direction, μm	Diameter along the 2 direction, μm
780.06	836.24
900.32	907.53

The analysis of the results obtained in the case of the set of the 1 SUD and 1 SUD TT samples highlighted the fact that the differences between the two samples are not that big, the wear intensity values being very close (minimum 2.617E-08 for the 1 SUD sample and 2.7858E-08 respectively for the 1 SUD TT sample; maximum 3.3082E-08 for the 1 SUD sample and

respectively $3.2001E-08$ for the 1 SUD TT sample). These results lead to the conclusion that the application of the heat treatment causes only a slight reduction in the wear resistance of the weld deposit with high entropy alloys.

The welded samples from the 2 batch, respectively 2 SUD and 2 SUD TT, were prepared in a similar way, the layout of the wear marks being shown in Fig. 6.6.

It can be seen that the diameter of the footprint is larger on the area corresponding to the base material, which indicates a lower value of wear resistance.

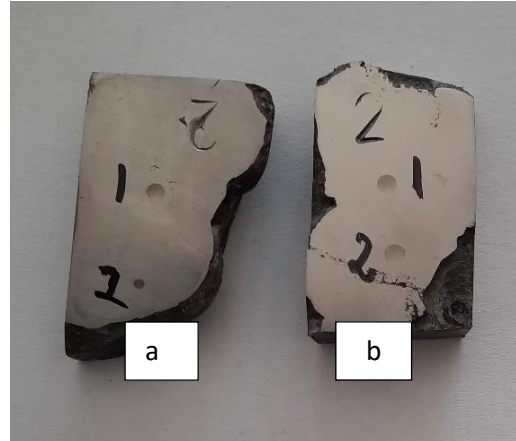


Fig. 6.6. Preparation of the samples from the 2 SUD batch for performing the wear test: a) 2 SUD sample; b) 2 TT sample.

Compared to the samples from the I set, in this case a lower wear resistance is found, expressed by higher wear intensity values (minimum $3.5459E-08$ for the 2 SUD sample and $1.4313E-07$ for the 2 SUD TT sample, respectively maximum $1.1157E-07$ for the 2 SUD sample and $1.5841E-07$ for the 2 SUD TT sample). And in this case, the application of heat treatment after welding caused a slight decrease in wear resistance. As a result, it can be said that heat treatment is not necessary even for this material deposited by welding, if an increase in wear resistance is desired.

The welded samples of the 3 batch, namely MB and MB TT were prepared similarly. This test was performed to compare the wear behavior of the base material and the weld deposit with the high entropy alloy from the AlCrFeNiMn system.

Based on these results, the important conclusion can be drawn that weld loading caused a significant increase in the wear resistance of the drill bit material, even in the absence of heat treatment.

After applying the heat treatment, a slight increase in the wear resistance of the base material was obtained, but not at the level recorded in the case of the weld loaded 1 SUD sample (minimum $3.7585E-08$ and maximum $4.2728E-08$).

Therefore, the general conclusion can be drawn that the application of heat treatment is not necessary to increase the wear resistance of the weld deposited material on the drill bits. In addition, this metallurgical procedure requires additional energy, time and labor work, which is not justified in this application.

6.2. CORROSION RESISTANCE TESTING OF ALLOYS WELD DEPOSITED ON DRILLING BIT STEEL

Corrosion resistance was estimated by the *linear polarization method*. Corrosion behavior in saline media with a 3.5% NaCl concentration was evaluated based on potentiodynamic curves, which were generated using VersaStudio v.2.50.3 software. The linear

polarization curves were plotted, the open circuit potential (E_{OC}) being recorded for 3 hours, in 3% NaCl solution at a temperature of 25 °C, as well as the potentiodynamic polarization curves (Tafel curves) for voltage values of -0.2 V (vs OCP) to +0.2 V (vs OCP), with a scan rate of 1 mV/s. The tests were carried out in a standard electrochemical cell, where a saturated calomel electrode (SCE) was used as a reference electrode, a platinum electrode as a recording electrode, and high-entropy alloy samples constituted the work electrode.

Based on the analysis of the value of the open circuit potential (E_{oc}), it can be said that the more electropositive values express a better corrosion behavior, it is seen that the HEA 5 sample has the lowest values of this parameter.

Under the corrosion potential's aspect (E_{cor}), a more electropositive value of the investigated material denotes a better corrosion behavior in the testing environment. Studying the values obtained for the investigated samples shows that the HEA 5 sample has the most electropositive value (-320 mV), which indicates a higher passivation rate compared to the other investigated samples. It is known that a reduced value of the corrosion current density (i_{cor}) corresponds to a better value of corrosion resistance. Based on this criterion, it is found that the HEA 1 alloy sample ($1.037\mu\text{A}/\text{cm}^2$) presents a better corrosion behavior.

From the analysis of the corrosion rate values (CR) obtained through electrochemical tests in 3.5% NaCl solution, results that the lowest values are obtained in the case of the HEA 1 sample, with the corrosion rate value of $10.81\mu\text{m}/\text{year}$ and respectively in the HEA 6 sample, of $15.62\mu\text{m}/\text{year}$. The HEA 5 sample shows the highest value of CR ($42.95\mu\text{m}/\text{year}$) consequently having the weakest corrosion behavior compared to the other investigated samples.

6.3. CONCLUSIONS REGARDING THE MECHANICAL AND CORROSION BEHAVIOR OF WELDED DEPOSITS FROM HIGH ENTROPY ALLOYS

- The wear resistance tests showed that the non-heat-treated base material shows wear intensity values around 2 times higher than those obtained in the case of the sample loaded by welding with alloys having high entropy
- The highest corrosion resistance values were obtained for the HEA 1 alloy, with the highest aluminium concentration (corrosion rate value of $10.81\mu\text{m}/\text{year}$) and in the case of the alloy with the lowest aluminium content (corrosion rate value of $15.62\mu\text{m}/\text{year}$).
- The weakest corrosion behavior was recorded by the HEA 5 alloy, with medium aluminium content (corrosion rate value of $42.95\mu\text{m}/\text{year}$).

CHAPTER VII. CONCLUSIONS AND CONTRIBUTIONS. FURTHER RESEARCH DIRECTIONS

7.3. PERSONAL CONTRIBUTIONS

Starting from the objectives proposed in the doctoral thesis, applying the new concepts regarding the design and obtaining of high-entropy alloys and analyzing the results of my theoretical and experimental research carried out within it, the personal contributions can be synthetically presented as follows:

7.3.1. Theoretical contributions

- Carrying out an in-depth documentary study regarding the stress conditions of drilling bits, the analysis of the causes that determine wear and tear, the identification of reconditioning procedures to increase the lifespan of their use;

7.3.2. Scientific contributions

- The design of high-entropy alloy recipes from the AlCoCrFeNi and AlCrFeNiMn alloy systems intended for the welding reconditioning of the drill bits, by changing the proportions of the alloying elements used, on the principle of ensuring the characteristics of wear resistance and associated corrosion resistance;
- Creation of experimental batches of high-entropy alloys using the vacuum electric arc melting process and the processing of the new metal alloys for the production of rods for weld loading;
- Elaboration and implementation of an experimental program for weld loading with the WIG method of drill bits using the high entropy alloys made;
- Carrying out thermal treatments, with different cooling regimes, applied to the samples taken from the drilling bits weld loaded with high entropy alloys;
- The study of the effects of their thermal treatments on the microstructural and hardness changes of the deposits made by welding with alloys having high entropy;
- Analysis of the quality of welded deposits with non-destructive methods (visual control, control with penetrant liquids)
- Carrying out mechanical tests to determine the service characteristics of the new high entropy alloys designed and made, including tests for wear resistance and determination of hardness (on each deposit microzone, compared to that of the drill bit material) under conditions of welding deposition or after applying thermal treatments;

7.4. FURTHER RESEARCH DIRECTIONS

- Development of new high entropy alloy recipes for heavy wear applications.
- Study of welding behavior of new high entropy alloys.
- Writing papers, didactic materials related to high entropy effects with applications in industry, participation in research teams with academic or industrial representatives to solve technical problems.

BIBLIOGRAPHY (extras)

- [1] *Georgescu G.*-Tehnologia forării sondelor, Editura Didactică și Pedagogică, București, 1983.
- [2] *S.C. Petrostar S.A. Ploiești* - Forajul sondelor, Carnet tehnic, 2000.
- [3] *Tatu G.* - Carnet tehnic. Forarea sondelor, Editura Tehnică, București, 1983.
- [4] *Olănescu M., Horhoianu G., Beca G.* - Forajul sondelor, Editura Didactică și Pedagogică, București, 1962.
- [5] https://upb.ro/wp-content/uploads/2020/03/olaru_mihai_rezumat_rom.pdf
- [6] *Slăniceanu V., Stoianovi G.* – Sape și scule pentru forajul sondelor, Editura Tehnică, București, 1964.
- [7] *Ivan S. , Botezatu V.* - Forajul sondelor- Manual Școala Profesională.
- [9] *Macovei N.*- Echipament de foraj, Editura Universitatea din Ploiești, 1996.
- [10] *Bolunduf I.L.*- Materiale și tehnologii neconvenționale, Editura Tehnică-info, Chișinău, 2012.
- [11] *V. Geantă, I. Voiculescu, B. Istrate, D. M. Vranceanu, R. Ciocoiu, C. M. Cotruț*-The Influence of Chromium Content on the Structural and Mechanical Properties of AlCr_xFeCoNi High Entropy Alloys, International Journal of Engineering Research in Africa Submitted: 2018, Vol. 37, pp 23-28.
- [12] *V. Geantă, T. Chereches, P. Lixandru, I. Voiculescu, R. Stefanoiu, D. Dragnea, T. Zecheru and L. Matache* - Virtual Testing of Composite Structures Made of High Entropy Alloys and Steel, , Metals 2017, 7, 496; doi:10.3390/met7110496.
- [13] *I. Voiculescu, V. Geantă, I.M. Vasile, R. Ștefănoiu, M. Tonoiu* - Characterisation of weld deposits using as filler metal a high entropy alloy, Journal of optoelectronics and advanced materials, Vol. 15, No. 7- 8, July – August 2013, p. 650 – 654.
- [14] *V. Geantă, I. Voiculescu, R. Ștefănoiu, D. Savastru, I. Csaki, D. Patrol, L. Leonat*-Processing and characterization of advanced multi-element high entropy materials from AlCrFeCoNi system, Optoelectronics and advanced materials– Rapid communications Vol. 7, No. 11-12, November - December 2013, p. 874-880.
- [27] *Petre M., Cristescu M.* – Forajul sondelor și extracția petrolului- Editura UPG din Ploiești, 2013.
- [28] *Gheorghiuțoiu M.* – Mic îndrumar de utilizare a sabelor de foraj- Editura UPG din Ploiești, 2010.
- [45] *Rakesh B. Nair, H.S. Arora, H.S. Grewal* -Microwave synthesized complex concentrated alloy coatings: Plausible solution to cavitation induced erosion-corrosion, Ultrasonics - Sonochemistry 50 (2019) 114–125.
- [46] *Steadyman Chikumba and Veeredhi Vasudeva Rao* - High-entropy alloy: challenges and prospects, th International Conference on Latest Trends in Engineering & Technology (ICLTET'2015) Nov. 26-27, 2015 Irene, Pretoria (South Africa).
- [47] *Daniel B. Miracle *, Jonathan D. Miller, Oleg N. Senkov, Christopher Woodward, Michael D. Uchic and Jaimie Tiley* - Exploration and Development of High Entropy Alloys for Structural Applications, Entropy 2014, 16, 494-525. doi: 10.3390 /e16010494.

- [48] Y.F. Ye, Q. Wang, J. Lu, C.T. Liu and Y. Yang - High-entropy alloy: challenges and prospects, *Materials Today* _ Volume 19, Number 6 _ July/August 2016.
- [50] Ming-Hung Tsai - Physical Properties of High Entropy Alloys, *Entropy* 2013, 15, 5338-5345; doi:10.3390/e15125338.
- [51] M. Claudia Troparevsky, James R. Morris, Paul R. C. Kent, Andrew R. Lupini and G. Malcolm Stocks - Criteria for Predicting the Formation of Single-Phase High-Entropy Alloys, *PHYSICAL REVIEW X* 5, 011041 (2015).
- [52] Daniel B. Miracle, Jonathan D. Miller, Oleg N. Senkov, Christopher Woodward, Michael D. Uchic and Jaimie Tiley - Exploration and Development of High Entropy Alloys for Structural Applications, *Entropy* 2014, 16, 494-525. doi:10.3390/e16010494, ISSN 1099-4300.
- [53] A.T. Samaeia, M.M. Mirsayarb and M.R.M. Alihac- The microstructure and mechanical behavior of modern high temperature alloys, 2015 Growing Science Ltd. doi: 10.5267/j.esm.2015.1.001.
- [146] Voiculescu, I., Geantă, V., Ștefănoiu, R., Patroi, D., Binchiciu, H., Influence of the Chemical Composition on the Microstructure and Microhardness of AlCrFeCoNi High Entropy Alloy. *Rev. Chim.*, Vol. 64, No. 12, 2013, p.1441-1444. ISI Thomson Reuters, IF = 1,122 (Q3). ISSN: 0034-7752.
- [147] Voiculescu, I., Geantă, V., Vasile, I.M., Ștefănoiu, R., Tonoiu, M., Characterisation of weld deposits using as filler metal a high entropy alloy. *Journal of Optoelectronics and Advanced Materials*, Vol. 15, No. 7-8, 2013, p.650 – 654. ISI Thomson Reuters, ISSN: 1454-4164.
- [148] Geantă, V., Voiculescu, I., Ștefănoiu, R., Savastru, D., Csaki, I., Patroi, D., Leonat, L., Processing and characterization of advanced multi-element high entropy materials from AlCrFeCoNi system. *Optoelectronics and advanced materials – Rapid Communications*, Vol. 7, 2013, p.874-880, ISSN: 1842-6573.
- [149] Ștefănoiu, R., Geantă, V., Voiculescu, I., Csaki, I., Ghiban, N., Researches regarding the influence of chemical composition on the properties of Al_xCrFeCoNi alloys. *Rev. Chim*, Vol. 65, No. 7, p. 819-821, (2014). ISI Thomson Reuters, ISSN: 0034-7752.
- [150] Geanta, V; Taca, M; Daisa, D; Voiculescu, I., Ștefănoiu, R, Constantinescu, DM, Savastru, D, Influence of the chemical composition on the mechanical properties of forged microalloyed steels, *Journal of Optoelectronics and Advanced Materials*, Vol. 17, Issue 7-8 (2015) p: 1004-1011, ISSN: 1454-4164, eISSN: 1841-7132. IDS Number: CP6AV.